P-09-14

Forsmark site investigation

Borehole KFM02B Characterisation of pore water

Part 1 Diffusion experiments and pore water data

H N Waber
Rock Water Interaction, University of Bern

J A T Smellie
Conterra AB

March 2009

Svensk Kärnbränslehantering AB
Swedish Nuclear Fuel
and Waste Management Co

Box 250, SE-101 24 Stockholm
Phone +46 8 459 84 00

ISSN 1651-4416
SKB P-09-14

Forsmark site investigation

Borehole KFM02B Characterisation of pore water

Part 1 Diffusion experiments and pore water data

H N Waber
Rock Water Interaction, University of Bern

J A T Smellie
Conterra AB

March 2009

Keywords: AP PF 400-05-126, Site investigations, Matrix pore water, Leaching, Diffusion, Chemistry, Palaeohydrogeology.

Abstract

Pore water investigations in borehole KFM02B were aimed at the characterisation of pore water and its implication to the palaeohydrogeological evolution of the hanging wall segment of the Forsmark site. Samples were collected specifically from deformation zones ZFMA2 and ZFMF1 close to water-conducting fractures, in addition to samples collected from the intact rock matrix at greater distances from any water-conducting fracture. Pore water has been extracted successfully from 39 samples by laboratory out-diffusion methods with half of them related to a water-conducting zone within deformation zone ZFMF1. The methodology to extract and analyse the pore water is outlined and the analytical data are tabulated. The data are critically reviewed for their significance with respect to *in situ* conditions.

The possible contamination of the core material by drilling fluid was investigated in borehole KFM02B by applying the same indirect extraction methods as previously employed (/Waber and Smellie, 2005, 2007/) to drillcores drilled with spiked drilling fluid. The results indicate that the contamination induced by stress release during drilling, and the drilling process itself, is less than about 8% of the obtained Cl^- concentration for the pore water, and thus well within the uncertainty band of the cumulated error of the applied experimental and analytical methods. Therefore, the produced data can be considered representative for *in situ* conditions.

The connected pore space in the core material of borehole KFM02B was measured on different types of originally saturated samples using two different, largely independent methods. The connectivity depends on the distance of the rock matrix sample to the next deformation/alteration zone, i.e. on the rock's texture and alteration state. Changes in the chemical and isotopic composition of the pore water coincide with changes in the hydrological regime, i.e. the fracture frequency and proximity to water-conducting fractures, which in turn reflect the different structural domains of deformation zones ZFMA2 (411–431 m) and ZFMF1 (462–512 m). The presence of large components of brackish marine water (i.e. Littorina and/or Baltic Sea water type) in the pore water alternates with cold-climate glacial type signatures in discrete zones related to conductive fractures down to 565 m borehole length. In general, the hanging wall bedrock intercepted by borehole KFM02B represents a dynamic hydraulic system where mainly geologically young groundwater signatures from glacial to present-day times are preserved. This contrasts with the findings previously observed for the footwall bedrock segment in the northwestern part of the Forsmark candidate area.

Summary

Pore water that resides in the pore space between minerals and along grain boundaries in crystalline rocks of low permeability cannot be sampled by conventional groundwater sampling techniques and therefore has to be characterised by applying indirect methods based on drillcore material. This requires a considerable logistic effort because the drillcore material must be preserved in its original saturated state from the time of drilling to the experiments carried out in the laboratory. Pore-water investigations in borehole KFM02B had three major objectives: a) the characterisation of pore water and its implication to the palaeohydrogeological evolution of the hanging wall segment area of the Forsmark site, b) the continuous sampling of a profile from a water-conducting zone into the adjacent intact rock matrix, and c) evaluation of the possible effects of stress release and drilling process on the generated pore water results. While objectives (a) and (c) could be fully accomplished, the continuous sampling of pore water samples did not commence close enough to the intended highly transmissive fracture because of the difficulty in predicting the depth of its interception during drilling. The methodology to extract and analyse the pore water is outlined and the analytical data are tabulated. The data are critically reviewed for their significance with respect to *in situ* conditions.

The possible contamination of the core material by drilling fluid was investigated in borehole KFM02B by applying the same indirect methods as previously employed (/Waber and Smellie, 2005, 2007/). However, in this case drilling was performed with spiked drilling fluid. This study revealed that the considerable logistic effort to sample drillcore material in its original saturated state was greatly worthwhile. The results indicate that for the rocks at Forsmark, the contamination induced by stress release during drilling, and the drilling process itself, is less than about 8% of the obtained Cl^- concentration for the pore water and is thus well within the uncertainty band of the cumulated error of the applied experimental and analytical methods. Therefore, the produced data can be regarded as representative for *in situ* conditions thus justifying their usage for palaeohydrogeological interpretation.

For the characterisation of pore water in the core material from borehole KFM02B, samples were collected specifically close to water-conducting fractures within the intersected deformation zones ZFMA2 (411–431 m borehole length) and ZFMF1 (485–512 m borehole length). One of the fractures was sampled just within the rock matrix at 430.74 m borehole length (ZFMA2) and the other one at 512.57 m borehole length (ZFMF1). Following the deepest borehole intersection of ZFMF1 with the underlying rock matrix, a continuous series of samples were taken from 512.57 to 517.34 m borehole length. At greater depths to the maximum borehole depth drilled (573.87 m), samples were collected from the intact rock matrix at distances greater than 5 m (if possible) from any water-conducting fracture.

Pore water has been extracted successfully from 39 samples by laboratory out-diffusion methods with half of them being related to a water-conducting zone within deformation zone ZFMF1 between about 500–530 m borehole length. The connected pore space in the core material of borehole KFM02B was measured on different types of originally saturated samples using two different, largely independent methods. The connectivity depends on the distance of the rock matrix sample to the next deformation/alteration zone, i.e. on the rock's texture and alteration state. For the large-sized intact drillcore samples used in the out-diffusion experiment, the water-loss porosity varies between 0.38–0.86 vol.% with an average 0.55 ± 0.10 vol.%, except for two tectonised samples with a water-loss porosity of 0.71 vol.% and 0.90 vol.%.

Pore water in the rocks of the hanging wall bedrock segment is generally of a dilute Na-HCO_3-Cl chemical type. Changes in the chemical and isotopic composition of the pore water coincide with changes in the hydrological regime, i.e. the fracture frequency and proximity to water-conducting fractures, which in turn reflect the different structural domains of deformation zones ZFMA2 and ZFMF1. Pore-water Cl^- concentrations are mainly below 1,500 mg/kg H_2O from

shallow to great depth. Higher Cl^- concentrations, up to a maximum of about 3,000 mg/kg H_2O, are related to discrete water-conducting fractures within deformation zones ZFMA2 and ZFMF1 and, in combination with the isotope composition and Mg^{2+} concentrations, indicate the presence of large components of brackish marine water (i.e. Littorina and/or Baltic Sea water types). Down to a depth of about 420 m the oxygen isotope signatures become increasingly depleted in ^{18}O and ^{2}H towards cold climate glacial-type signatures. In discrete zones related to conductive fractures, such depleted ^{18}O and ^{2}H signatures associated with the lowest Cl^- concentrations occur down to 565 m indicating that in these fractures cold climate glacial-type groundwaters must have circulated prior to the groundwater sampled today. In general, the hanging wall bedrock intercepted by borehole KFM02B represents a hydraulically dynamic system where mainly geologically young signatures from glacial to present-day times are preserved. This is in contrast with findings previously observed and described for the footwall bedrock in the northwestern part of the Forsmark candidate area.

Sammanfattning

Porvatten som finns i porer mellan mineraler och längs korngränser i kristallint berg av låg permeabilitet kan inte provtas med konventionella provtagningstekniker för grundvatten och måste karakteriseras med hjälp av indirekta metoder baserade på material från borrkärnor. Detta kräver betydande logistiska insatser eftersom borrkärneproven måste bevaras i sina ursprungliga mättade tillstånd från borrningstillfället till dess att experimenten utförs i laboratoriet. Porvatten-undersökningarna i borrhålet KFM02B hade tre huvudsakliga syften: a) karakterisering av porvatten och tolkning av porvattenresultatens implikationer på den paleohydrogeologiska utvecklingsmodellen i hängväggssegmentet inom undersökningsområdet i Forsmark, b) kontinuerlig provtagning av en profil från en vattenförande zon in i den omgivande intakta bergmatrisen, och c) utvärdering av möjliga effekter, orsakade av tryckavlastning av berget i samband med borrning och av borrningsprocessen i sig, på de genererade porvattenresultaten. Målen (a) och (c) kunde uppnås fullständigt men den kontinuerliga provtagningen av porvattenprov (borrkärna) påbörjades inte så nära den högtransmissiva sprickan som var avsett på grund av svårigheter att förutsäga var sprickzonen skulle påträffas under borrningen. Metodologin för att extrahera och analysera porvatten beskrivs i rapporten och data presenteras. Datas signifikans med avseende på *in situ* förhållanden granskas också kritiskt.

Möjlig spolvattenkontaminering av borrkärnematerialet undersöktes i borrhål KFM02B genom att använda samma indirekta metoder på borrkärnor som tidigare tillämpats. I detta fall utfördes dock borrningen med specialmärkt spolvatten. Denna studie avslöjade att de logistiska ansträngningar som gjorts för att ta prov från borrkärnor i deras ursprungliga mättade tillstånd var värda besväret. Resultaten indikerar att kontamineringen av borrkärna från berget i Forsmark orsakade av tryckavlastningen och av själva borrningsprocessen är mindre än omkring 8 % av den erhållna kloridkoncentrationen för porvattnet. Detta ligger väl inom den osäkerhet som motsvarar det ackumulerade felet för de experiment- och analysmetoder som har tillämpats. Därför kan producerade data betraktas som representativa för *in situ* förhållandena vilket berättigar deras användning för palaeohydrogeologisk tolkning.

Från borrhål KFM02B togs prov specifikt för karakterisering av porvatten från kärnmaterial i närheten av vattenförande sprickor inom deformationszonerna ZFMA2 (411–431 m) och ZFMF1 (485–512 m) som korsas vid omkring 420 m och 495 m borrhålslängd. Vidare togs prov från intakt berg på minst 5 m avstånd från närmsta vattenförande spricka. Porvatten har framgångsrikt extraherats från 39 prov med laboratoriemetoder som bygger på utdiffusion. Hälften av proven var relaterade till en vattenförande zon inom deformationszonen ZFMF1 mellan 500–530 m borrhålslängd. Den konnekterade porvolymen i kärnmaterialet från borrhål KFM02B mättes på olika typer av ursprungligen mättade prov med hjälp av två olika och huvudsakligen oberoende metoder. Konnektiviteten beror på avståndet mellan bergmatrisprovet och nästa deformationszon/omvandlade zon, dvs på bergtexturen och omvandlingsgraden. För de stora intakta borrkärneproven som användes i utdiffusionsexperimenten varierade vatten-förlustporositeten mellan 0.38–0.86 vol.% med ett medelvärde på 0.55 ± 0.10 vol.%, utom för två tektoniserade prov med en vattenförlustporositet på 0.71 vol.% respektive 0.90 vol.%.

Porvattnet i berget inom hängväggssegmentet representerar generellt en utspädd Na-HCO_3-Cl vattentyp. Förändringar i kemisk sammansättning och isotopsammansättning sammanfaller med förändringar i hydrogeologisk regim, vilka är avhängiga sprickfrekvensen och närheten till vattenförande sprickor, som i sin tur reflekterar olika strukturella domäner av deformations-zonerna ZFMA2 and ZFMF1. Porvattnens kloridkoncentrationer är huvudsakligen lägre än 1 500 mg/kg H_2O från grunda till stora djup. De högre kloridkoncentrationer som påträffats, upp till maximalt omkring 3 000 mg/kg H_2O, är relaterade till diskreta vattenförande sprickor inom deformationszonerna ZFMA2 and ZFMF1. I kombination med isotopsammansättning och magnesiumkoncentrationer indikerar den högre koncentrationen närvaron av en stor andel bräckt marint vatten (t ex Littorina och/eller Östersjövatten). Ner till ett djup på ungefär 420 m

blir isotopsignaturerna mer och mer fattiga på ^{18}O and ^{2}H och förändras mot signaturer typiska för kallt klimat, vilket indikerar inslag av grundvatten av glacial typ. I diskreta zoner relaterade till vattenförande sprickor förekommer denna typ av låga ^{18}O and ^{2}H signaturer, kopplade till några av de lägsta observerade kloridkoncentrationerna, ner till 565 m vilket indikerar att glacialt grundvatten härrörande från en period med kallt klimat måste ha uppehållit sig i sprickorna innan det ersattes av det grundvatten som vi provtar idag. Generellt representerar hängväggen, genomkorsad av KFM02B, ett dynamiskt hydrauliskt system där huvudsakligen unga signaturer från glacial tid till nutid har bevarats. Detta kontrasterar mot tidigare iakttagelser som gjorts och som beskrivits för berget i liggväggen inom den nordvästra delen av Forsmarks kandidatområde.

Contents

1 Introduction

This document reports the performance and results of the activity *characterisation of pore water* in drillcore samples within the site investigation programme at Forsmark. The drillcore samples were selected during drilling of borehole KFM02B in accordance with activity plan AP PF 400-05-126.

Crystalline rocks are characterised in general by two hydraulic regimes. The first regime includes the water-conducting zones related to regional or local fracture networks. The second regime includes the bedrock mass of low permeability between the water-conducting zones. The mass of pore water contained in the low-permeability matrix of the crystalline rock at Forsmark is significant compared to the mass of groundwater circulating in the fractures, and therefore its influence on the fracture groundwater and a future deep repository needs to be understood. The interaction between pore water in the low permeable bedrock and groundwater in transmissive fractures depends on the degree of connectivity of the pore system, where solute transport can take place in the pore water, and on the differences in the chemical composition between the two systems. Pore water and fracture groundwater always tend to reach chemical and isotopic equilibrium given a long enough period of stable conditions. Thus, the pore water acts either as a sink or a source for solutes depending on the concentration gradient established between pore water and fracture groundwater, and therefore becomes an archive of past fracture-groundwater compositions and the palaeohydrogelogical history of a site.

In addition, since repository construction will be restricted largely to bedrock of low permeability, this pore water over time will interact with the repository barrier materials (e.g. bentonite; canister) potentially leading to a deterioration in their physical properties. For safety assessment considerations it is therefore important to know the composition of such pore water and its evolution over recent geological time, certainly during the last thousands to hundreds of thousands of years in accordance with the expected lifespan of a repository.

Pore water compositions can be assessed by combining the information gained from pore water profiles within bedrock of low permeability and the chemical and isotopic data of formation groundwaters circulating in the adjacent fracture zones. However, pore water that resides in the pore space between minerals and along grain boundaries in crystalline rocks of low permeability cannot be sampled by conventional groundwater sampling techniques and therefore has to be characterised by applying indirect methods based on drillcore material. The success of pore water investigations relies on obtaining the originally saturated rock material. This requires freshly drilled cores from boreholes and the immediate on-site conditioning of such material within minutes after drillcore recovery (see /Waber and Smellie 2008b/ for details). In addition, rather large-sized core samples are required to compensate for the low pore water content and to minimise possible artefacts induced from the time of drilling to the time of analysis.

Previously during the SKB Site investigation programmes such techniques were successfully applied at Forsmark /Waber and Smellie 2005, 2007/ and at Laxemar /Waber and Smellie 2006abc, 2008a/ to trace the pore water chemistry in low permeable bedrock to depths of around 1,000 m.

These investigations revealed that pore water data obtained for a single sample from a borehole can only be interpreted to a limited degree. Therefore, borehole KFM02B was selected to sample a small-scale profile extending several metres from a water-conducting fracture into the host rock matrix, in addition to the profile systematically sampled along the complete borehole length. These two sets of data are then compared to the present-day fracture groundwater compositions characterising the closest water-conducting fracture to the selected pore water samples. In addition, the last section of the borehole was drilled with traced drilling fluid to investigate possible contamination of pore water samples by drilling fluid.

This report presents the methodologies employed, a compilation of the resulting analytical data from the various experiments, and the derived pore water data.

2 Hydrogeological Setting

Borehole KFM02B was drilled from drill site 2 in the south-east sector of the candidate area in the hanging wall bedrock in fracture domain FFM03, and maximum penetration was into the underlying footwall (Figures 2-1 and 2-3). The objectives of the borehole were: a) to confirm or otherwise the existence of two gently-dipping deformation zones ZFMA2 and ZFMF1 and investigate their effect on the local stress field, b) to conduct cross-borehole tracer tests, c) to sample a continuous profile away from a water-conducting zone into the surrounding rock matrix either in deformation Zone ZFMA2 or ZFMF1 for matrix pore water investigations, and d) to investigate the effects of possible drilling fluid contamination on pore water samples. This last-mentioned objective was carried out by using spiked drilling fluid during drilling of the last approximate 15 m of the borehole in the footwall in fracture domain FFM01.

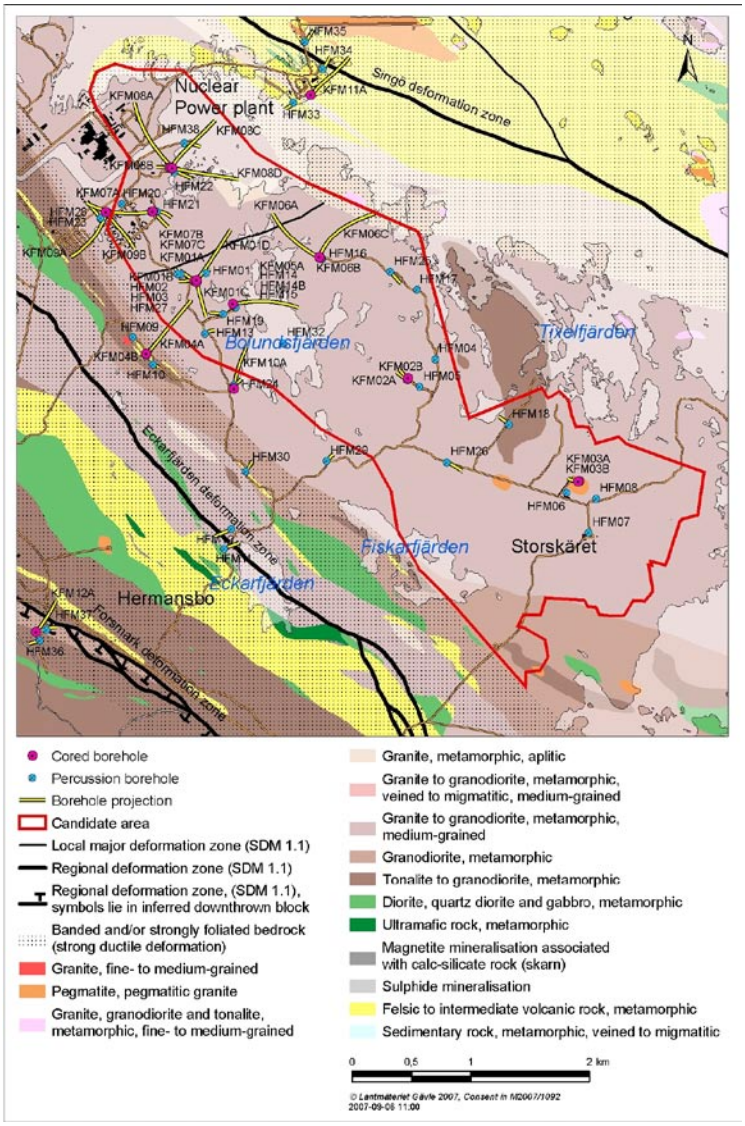

Figure 2-1. *Generalised geological map of the Forsmark site investigation area and the projection of borehole KFM02B (centre of map) used for pore water characterisation.*

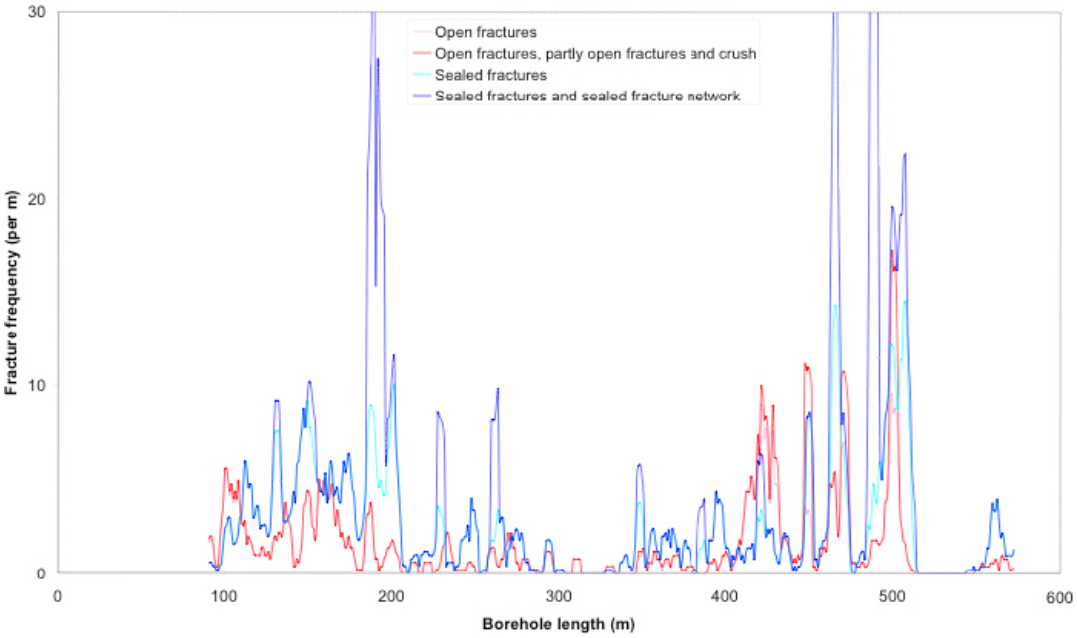

Figure 2-2. *Borehole KFM02B: Fracture frequency as a function of borehole length and expressed as moving average with a 5 m window and 1 m steps (from /Carlsten et al. 2007/). Note the distinct high frequency of open fractures between about 100–200 m and 400–500 m borehole length.*

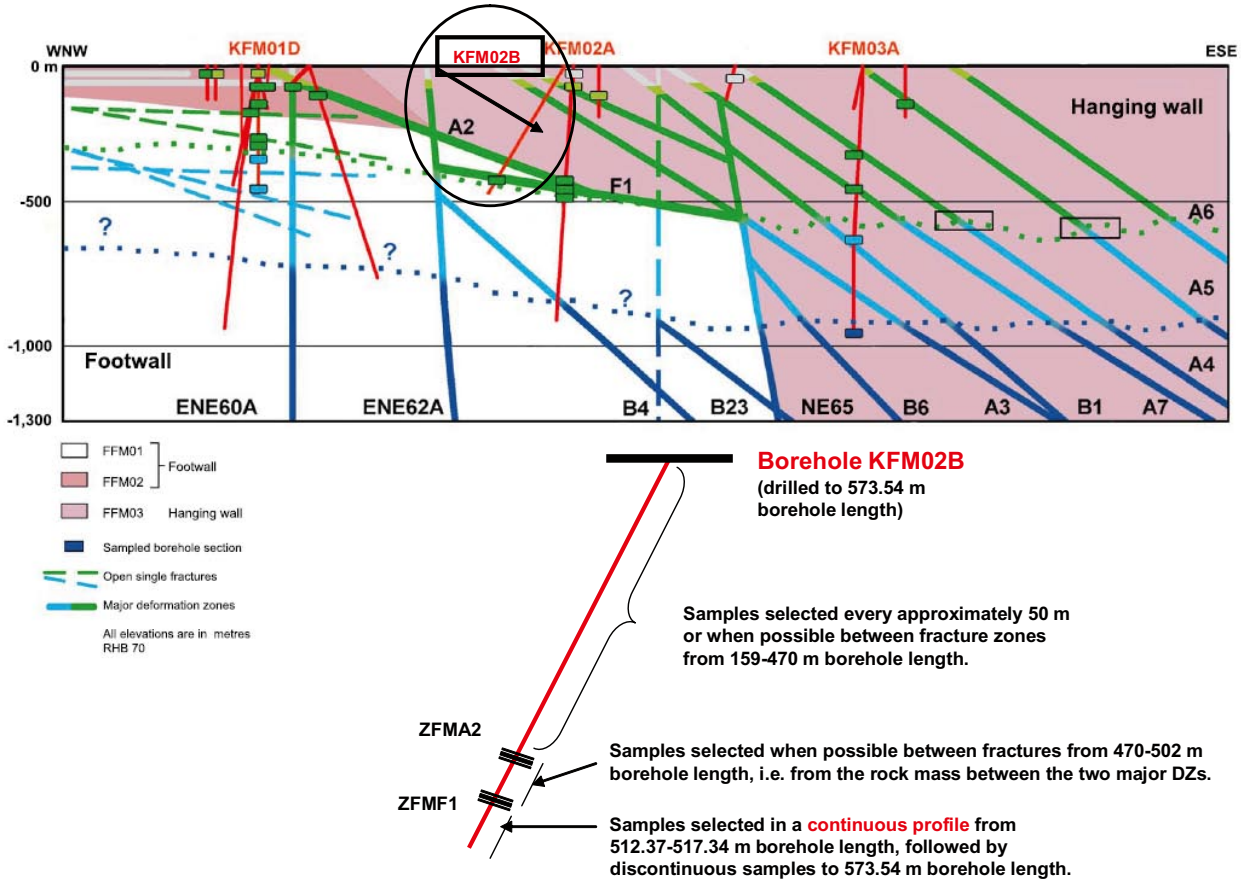

Figure 2-3. *Location of borehole KFM02B with respect to the hanging wall and footwall and to the major gently-dipping deformation zones ZFMA2 and ZFMF1. Also indicated are the locations of the pore water samples collected along the borehole length of KFM02B.*

Core drilling of borehole KFM02B commenced in early June 2006 and was halted at selected intervals for rock stress measurements and hydraulic monitoring. Continuous drilling started again in mid-December 2006 and the borehole was completed on February 13, 2007. It was drilled to a borehole length of 573.87 m at an inclination of 80.27° from the horizontal plane at ground level. The borehole was drilled using a telescopic drilling technique, where the first 87 m interval was percussion drilled and cased. Below 88.61 m the borehole was core-drilled with a diameter of 76 mm giving rise to a drillcore diameter of 50 mm.

The geology of borehole KFM02B is characterised by two rock units denoted as RU1 and RU2 (323–429 m) with the latter unit being sandwiched in-between two sections of the first one (RU1a from 88–323 m and RU1b from 429–537 m). The dominant rock types encountered are a fine- to medium-grained, lineated metagranite-granodiorite (rock type 101057) that comprises about 59% of the drillcore /Samuelsson et al. 2007, Carlsten et al. 2007/. Pegmatitic granite (101061) comprises about 19% and a lineated fine- to medium-grained granite (101058) about 14% of the drillcore. Over the entire drillcore are present only small amounts of amphibolite (102017, ~3.5%), fine- to medium-grained metagranitoid (~2.7%) and medium-grained metadiorite-gabbro (~1.4%). All other rock types contribute less than 1% of the drillcore (aplitic metagranite, quartz-dominated hydrothermal veins, calc-silicate rock and felsic to intermediate metavolcanic rock).

All rocks have experienced Svecofennian metamorphism under amphibolite facies conditions /Samuelsson et al. 2007/. Rock foliation is frequently developed leading to a distinct anisotropy and to a gneissic appearance of most of the core sections. Six zones with increased brittle deformation and an accumulation of closed and/or open fractures occur between 98–115 m, 145–204 m, 411–431 m, 447–451 m, 461–473 m, and 485–512 m borehole length (Figure 2-2, /Carlsten et al. 2007/). The crushed sections at 449 m and 471 m borehole length are highly altered, containing clay minerals, hematite and calcite. The remaining crush sections contain chlorite, clay minerals, calcite, prehnite and also epidote. Pyrite occurs rarely below about 400 m, while oxidised iron phases (hematite, iron hydroxides) are present throughout and are abundant in the tectonised zones.

At about 411–431 m borehole length, borehole KFM02B intersected deformation zone ZFMA2 and around 462–512 m it intersected deformation zone ZFMF1 (Figure 2-3). In the intervals between 461–473 m in ZFMA2 and 485–512 m in ZFMF1, distinct high frequencies of open fractures and crushed zones were observed. Based on these observations, the sample intervals for pore water samples were reduced from 470 m downwards and a continuous profile of pore water samples was collected starting at 512 m borehole length. Unfortunately, this was already about 10 m away from the water-conducting zone initially planned, as shown later by the differential flow logging, and underlines the difficulty of accurately predicting the intersection depths of deformation zones prior to drilling.

From differential flow logging of borehole KFM02B, a high frequency of highly transmissive fractures (up to $x \cdot 10^{-5}$ m^2/s) were observed between 86–126 m and 411–431 m borehole length /Väisäsvaara and Pöllänen 2007/. High transmissivities of more than 10^{-5} m^2/s were also observed in the highly deformed zones between 461–473 m and 485–512 m, but here mainly restricted to discrete inflow points at 470–471 m and 500–501 m borehole lengths.

Differential flow logging was concluded at 568 m borehole length without identifying the inflow points between 558–569 m which correspond to the first section drilled with spiked drilling fluid. Neither geological nor hydrological borehole logging is available for the last 6 m of the borehole.

3 Materials and methods

3.1 Samples and sample preparation

Between September 20th and February 13th 2006, a total of 43 samples were collected for pore water characterisation (Figure 2-3). Drillcore sections of about 20–40 cm in length were taken at regular depth intervals of about 50 metres from a borehole length of 159 m downwards. At about 470 m the sampling intervals were reduced based on the observation of the highly deformed zone between 461–473 m. A continuous profile of pore water samples, the so-called fracture profile, was collected starting at about 512 m borehole length and extending to about 517 m. Further downwards the sampling intervals were again increased to a few metres and this continued to the end of the borehole. As later shown by the differential flow logging, the fracture profile unfortunately started at a depth of about 12 m beyond the correct position which coincided with the water-conducting fracture of interest, i.e. a fracture with a transmissivity of more than 10^{-5} m^2/s /Väisäsvaara and Pöllänen, 2007/. However, some core sections were taken from this 12 m borehole length as part of the overall systematic sampling protocol (Figure 2-3).

The last five pore water samples collected from the final 559–573 m length of borehole KFM02B were drilled using drilling fluid that was spiked with 1 g iodine (added as NaI). This experiment was conducted to investigate the potential effects of stress release of the rock on the pore water samples during drilling. Both processes (i.e. stress release and drilling) could potentially result in an increase of the *in situ* connected porosity leading to a contamination of the *in situ* pore water and thus modify the results of the diffusion experiments. It was attempted to identify the degree of such possible contamination using iodine as a tracer.

An important requirement for pore water characterisation using rock samples is the preservation of the fully water-saturated state of the rock material immediately following drilling and sampling and during transportation from the site to the laboratory. This precaution is to inhibit possible water-rock interactions induced by exposure of the rock sample to air. To minimise these potential perturbing effects the samples were immediately wiped clean with a dry towel following drilling and selection, wrapped into a heavy-duty PVC bag, which was repeatedly flushed with nitrogen, evacuated and heat sealed. This procedure was repeated with a second PVC bag and finally sealed in a plastic coated Al-foil. The samples were then air freighted to the laboratory at the University of Bern, Switzerland, where they were immediately stored at 4°C in a cooling room and prepared for the various measurements and experiments within about 20 hours after arrival.

Once exposed to the air and/or stored over too long a time period, the drillcore samples lose their value for pore water characterisation. Therefore, the samples received had to be rapidly conditioned so that the different laboratory experimental procedures could be initiated. Based on on-site drillcore inspection, the use of available drillcore mapping information, BIPS logs and also hydraulic data from down-hole differential flow measurements, it was decided to analyse for all samples the chemical composition of the out-diffusion experiment solutions and the water isotope composition of the diffusive isotope exchange experiments, except for samples 3B-35 to 2B-38.

For legibility reasons, the sample labelling adopted in this report is a subsequent numbering of the samples with depth using the borehole name as prefix; similar labelling was used for the laboratory studies. Table 3-1 gives the list of samples used for pore water characterisation including their SKB number, the sample numbering used in this report, and the experiments and analyses performed on each sample. The general rock type, the distance of the sample to the next tectonised zone and the frequency of open fractures /Samuelsson et al. 2007/ in the near-vicinity of each sample are given in Table 3-2.

Table 3-1. KFM02B borehole: List of samples used for pore water studies and experiments and measurements performed.

Sample No	SKB Sample No	Average borehole length (m) [1]	Average elevation (m RHB 70)	Water-loss porosity	Density	Isotope equil. method	Chemistry out-diffusion experiments		
								$^{87}Sr/^{86}Sr$	Cl time-series
KFM02B-1	SKB 012400	158.91	–149.20	X	X	–	X	X	O
KFM02B-2	SKB 012401	171.83	–161.94	X	X	X	X	X	X
KFM02B-3	SKB 012402	210.64	–200.21	X	X	X	X	O	O
KFM02B-4	SKB012403	287.16	–275.64	X	X	X	X	X	X
KFM02B-5	SKB012404	393.29	–380.24	X	X	X	X	X	O
KFM02B-6	SKB012405	430.74	–417.14	X	X	X	X	X	X
KFM02B-7	SKB012406	441.45	–427.68	X	X	X	X	X	X
KFM02B-8	SKB012407	448.06	–434.19	X	X	X	X	X	X
KFM02B-9	SKB012408	459.84	–445.79	X	X	X	X	X	X
KFM02B-10	SKB012409	474.07	–459.79	X	X	X	X	X	O
KFM02B-11	SKB012410	478.89	–464.54	X	X	X	X	X	O
KFM02B-12	SKB012411	490.46	–475.92	X	X	X	X	X	X
KFM02B-13	SKB012412	498.84	–484.16	X	X	X	X	X	O
KFM02B-14	SKB012413	509.81	–494.95	X	X	X	X	X	X
KFM02B-15	SKB012414	512.57	–497.66	X	X	X	X	X	X
KFM02B-16	SKB012415	512.96	–498.04	X	X	X	X	X	O
KFM02B-17	SKB012416	513.34	–498.41	X	X	X	X	X	X
KFM02B-18	SKB012417	513.68	–498.75	X	X	X	X	O	O
KFM02B-19	SKB012418	514.04	–499.11	X	X	X	X	O	O
KFM02B-20	SKB012419	514.47	–499.50	X	X	X	X	X	X
KFM02B-21	SKB012420	514.84	–499.89	X	X	X	X	O	O
KFM02B-22	SKB012421	515.19	–500.23	X	X	X	X	O	X
KFM02B-23	SKB012422	515.54	–500.58	X	X	X	X	O	O
KFM02B-24	SKB012423	515.85	–500.89	X	X	X	X	X	X
KFM02B-25	SKB012424	516.12	–501.15	X	X	X	X	O	O
KFM02B-26	SKB012425	516.42	–501.44	X	X	X	X	O	X
KFM02B-27	SKB012426	516.72	–501.74	X	X	X	X	O	O
KFM02B-28	SKB012427	517.03	–502.04	X	X	X	X	O	X
KFM02B-29	SKB012428	517.34	–502.34	X	X	X	X	O	O
KFM02B-30	SKB012435	519.54	–504.51	X	X	X	X	X	X
KFM02B-31	SKB012443	522.11	–507.04	X	X	X	X	O	O
KFM02B-32	SKB012444	522.39	–507.31	X	X	X	X	X	X
KFM02B-33	SKB012458	527.55	–512.38	X	X	X	X	O	O
KFM02B-34	SKB012471	532.44	–517.19	X	X	X	X	X	X
KFM02B-35	SKB012492	540.40	–525.01	–	–	–	–	–	–
KFM02B-36	SKB012498	549.66	–534.11	–	–	–	–	–	–
KFM02B-37	SKB012499	554.17	–538.54	–	–	–	–	–	–
KFM02B-38	SKB012600	556.43	–540.75	–	–	–	–	–	–
KFM02B-39	SKB012601	559.83	–544.09	X	X	X	X	O	X
KFM02B-40	SKB012603	562.47	–546.69	X	X	X	X	X	X
KFM02B-41	SKB012604	565.29	–549.46	X	X	X	X	O	X
KFM02B-42	SKB012605	569.35	–553.45	X	X	X	X	O	X
KFM02B-43	SKB012607	573.65	–557.67	X	X	X	X	X	X

[1] Borehole inclination: approx 80°; borehole length values represent preliminary borehole data when sampled in the field.
X = Experiment performed, analytical data available.
P = Experiment performed, analytical data pending.
O = Experiment performed, analytical data not completed according to activity plan PF-400-05-126.
– = No experiment performed.

Table 3-2. KFM02B borehole: Sample geology and distance to alteration/ tectonisation.

Sample No	Average bore-hole length (m)	Lithology	Alteration /tectonisation [1)]	Fracture intensity [1)]
KFM02B-1	158.91	metagranite-granodiorite, homog. m-g, lineated	± 5 m	high
KFM02B-2	171.83	metagranite-granodiorite, homog. m-g, lineated	± 5 m	high
KFM02B-3	210.64	metagranite-granodiorite, homog. m-g, lineated	± 10 m	mod.
KFM02B-4	287.16	metagranite-granodiorite, homog. m-g, lineated	± 10 m	low
KFM02B-5	393.29	granite, homog. fine to medium-grained	± 20 m	low
KFM02B-6	430.74	metagranite-granodiorite, homog. m-g, lineated	± 5 m	high
KFM02B-7	441.45	metagranite-granodiorite, homog. m-g, lineated	± 10 m	low
KFM02B-8	448.06	metagranite-granodiorite, homog. m-g, lineated	± 20 m	low
KFM02B-9	459.84	metagranite-granodiorite, homog. m-g, lineated	± 10 m	mod.
KFM02B-10	474.07	metagranite-granodiorite, homog. m-g, lineated	± 5 m	mod.
KFM02B-11	478.89	metagranite-granodiorite, homog. m-g, lineated	± 10 m	mod.
KFM02B-12	490.46	metagranite-granodiorite, homog. m-g, lineated	± 10 m	high
KFM02B-13	498.84	metagranite-granodiorite, homog. m-g, lineated	± 5 m	high
KFM02B-14	509.81	metagranite-granodiorite, homog. m-g, lineated	± 5 m	high.
KFM02B-15	512.57	metagranite-granodiorite, homog. m-g, lineated	*± 5 m [2)]*	*high [2)]*
KFM02B-16	512.96	metagranite-granodiorite, homog. m-g, lineated	*± 5 m [2)]*	*high [2)]*
KFM02B-17	513.34	metagranite-granodiorite, homog. m-g, lineated	*± 5 m [2)]*	*high [2)]*
KFM02B-18	513.68	metagranite-granodiorite, homog. m-g, lineated	*± 5 m [2)]*	*high [2)]*
KFM02B-19	514.04	metagranite-granodiorite, homog. m-g, lineated	*± 5 m [2)]*	*high [2)]*
KFM02B-20	514.47	metagranite-granodiorite, homog. m-g, lineated	*± 5 m [2)]*	*high [2)]*
KFM02B-21	514.84	metagranite-granodiorite, homog. m-g, lineated	*± 5 m [2)]*	*high [2)]*
KFM02B-22	515.19	metagranite-granodiorite, homog. m-g, lineated	*± 5 m [2)]*	*high [2)]*
KFM02B-23	515.54	metagranite-granodiorite, homog. m-g, lineated	*± 5 m [2)]*	*high [2)]*
KFM02B-24	515.85	metagranite-granodiorite, homog. m-g, lineated	*± 5 m [2)]*	*high [2)]*
KFM02B-25	516.12	metagranite-granodiorite, homog. m-g, lineated	*± 5 m [2)]*	*high [2)]*
KFM02B-26	516.42	metagranite-granodiorite, homog. m-g, lineated	*± 5 m [2)]*	*high [2)]*
KFM02B-27	516.72	metagranite-granodiorite, homog. m-g, lineated	*± 5 m [2)]*	*high [2)]*
KFM02B-28	517.03	metagranite-granodiorite, homog. m-g, lineated	*± 5 m [2)]*	*high [2)]*
KFM02B-29	517.34	metagranite-granodiorite, homog. m-g, lineated	*± 5 m [2)]*	*high [2)]*
KFM02B-30	519.54	metagranite-granodiorite, homog. m-g, lineated	*± 5 m [2)]*	*mod. [2)]*
KFM02B-31	522.11	metagranite-granodiorite, homog. m-g, lineated	*± 10 m*	*mod. [2)]*
KFM02B-32	522.39	metagranite-granodiorite, homog. m-g, lineated	*± 10 m*	*mod. [2)]*
KFM02B-33	527.55	metagranite-granodiorite, homog. m-g, lineated	*± 10 m*	*mod. [2)]*
KFM02B-34	532.44	metagranite-granodiorite, homog. m-g, lineated	*± 10 m*	*low [2)]*
KFM02B-39	559.83	metagranite-granodiorite, homog. m-g, lineated	*n.a. [2)]*	*mod. [2)]*
KFM02B-40	562.47	metagranite-granodiorite, homog. m-g, lineated	*n.a. [2)]*	*mod. [2)]*
KFM02B-41	565.29	metagranite-granodiorite, homog. m-g, lineated	*n.a. [2)]*	*low [2)]*
KFM02B-42	569.35	metagranite-granodiorite, homog. m-g, lineated	*n.a. [2)]*	*low [2)]*
KFM02B-43	573.65	metagranite-granodiorite, homog. m-g, lineated	*n.a. [2)]*	*low [2)]*

[1)] Approximate distance to next major alteration zone and fracture intensity above and below sample (from WellCAD image, /Samuelsson et al. 2007/).

[2)] No geological drillcore log available; assumed based on fracture frequency plot /Carlsten et al. 2007/ and differential flow logging /Väisäsvaara. and Pöllänen 2007/; n.a. = not available.

Borehole length values represent preliminary borehole data when sampled in the field.

Following arrival at the laboratory the core sections were cut by dry sawing into full diameter samples of about 19 cm length to be used specifically for the out-diffusion experiments. In several cases the length of drillcore obtained was too short and this required an adjustment of the experimental set-up to accommodate core pieces of 12 cm length instead. The only observed drawback of this shorter sample length is the smaller volume of experiment solution obtained that does not allow all planned isotope analyses to be carried out. The remaining material from the top and bottom of the core section was used for the diffusive isotope equilibration method and the determination of the water content. The wet weight of such material was determined immediately after unpacking and preparation.

3.2 Analytical methods

Most of the analytical work of this study has been conducted at the Institute of Geological Sciences, University of Bern, Switzerland. Thus, if not otherwise stated the analytics have been performed at this institution.

3.2.1 Water content and water-loss porosity

The water content was determined by the gravimetric determination of the water loss by drying sub-samples at 105ºC until stable weight conditions (±0.002 g). Such sub-samples included drillcore material specifically designated to water-content measurements, the material used for the diffusive isotope-exchange method, and the large-sized drillcore sections used for the out-diffusion experiments.

If the material received allowed it, then the weight of the samples specifically designated to water-content measurements was chosen to be as large as possible to minimise possible desaturation effects and to account for variations in the grain size of the rocks. For the same reasons, intact drillcore pieces were used without creating unnecessary new surfaces by cutting and/or breaking. For some samples, however, the material was limited and the sample weight ranged from 90–300 g. Samples used for the diffusive isotope exchange experiments remained saturated throughout the experiment because they were placed in a vapour-tight vessel at 100% humidity during the equilibration procedure (see also below). The mass of samples available for these experiments varied between about 180–380 g. The most reliable water-content data are obtained from the large-sized drillcore sections used for the out-diffusion experiments. The mass of these intact core sections ranged between approximately 580–1,000 g and the difference in mass before (i.e. at the time of receiving the sample in lab) and after (i.e. after more than 100 days of immersion in the test water) the out-diffusion experiment was less than 0.1 permil for all samples. It is important to note that drying to stable-weight conditions of such large-sized samples lasts several months.

A measure for the bulk wet density, $\rho_{bulk,\,wet}$, of the rocks was obtained from the volume and saturated mass of the core samples used for out-diffusion experiments. The volume was calculated from measurements of height and diameter of the core samples using a Vernier calliper with an error of ± 0.01 mm. Variations in the core diameter over the lengths of the samples was found to be less than 0.05 mm for most samples and a constant diameter was used in the calculation of the volume. For the derived wet bulk density this results in an error of less than 3%.

The water-loss porosity, Φ_{WL}, was calculated using the water content and the bulk wet density according to:

$$\Phi_{WL} = WC_{wet} \cdot \frac{\rho_{bulk,wet}}{\rho_{water}} \qquad \text{(Eq. 3-1)}$$

A density of unity was assumed for the water density, ρ_{water}, based on the low to moderate salinity obtained for pore water in rocks of other boreholes from the Forsmark site (e.g. /Waber and Smellie 2005 and 2007/).

3.2.2 Isotope composition, $\delta^{18}O$ and $\delta^{2}H$, of pore water

The stable isotope composition of the pore water, $\delta^{18}O$ and $\delta^{2}H$, was determined by the diffusive isotope equilibration technique (see /Waber and Smellie 2005, 2006b/ for details and references). In this technique, the pore water isotope composition is derived indirectly by isotopic exchange between the pore water and test water of known composition. The isotope exchange occurs via the vapour phase without any direct contact between the rock sample and the test water. Rock pieces of about 1 cm in diameter from the centre of the core and a small petri dish filled with test water are stored together in a vapour-tight glass container. The mass and stable water isotope compositions of the test water are known. The water activity of the test water is slightly reduced by adding about 0.3 mol NaCl in order to lower the vapour pressure above the test-water surface, and thus to minimise loss of test water from the petri dish and condensation on the rock fragments and the glass container walls. The petri dish with the test water and the whole container are weighed before and after the exchange experiment to check that no water is lost from the container and that there occurred no transfer of test water to the sample by possible sorption on the rock material. Isotopic equilibrium in this system is achieved in about 20 to 30 days at room temperature depending on the size of the rock pieces, and the water content and water diffusivity of the rock. After complete equilibration, the two test waters were removed and analysed by conventional ion-ratio mass spectrometry at Hydroisotop GmbH, Germany. The results of the test solutions are reported relative to the V-SMOW standard with a precision of ±0.15‰ for $\delta^{18}O$ and ±1.5‰ for $\delta^{2}H$.

The diffusive isotope equilibration method was originally designed for rocks with water contents in the order of several percent. To account for the much lower water content in the crystalline rocks from the Forsmark area, the method was modified in that an artificial test water was used, which is strongly enriched in ^{2}H and depleted in ^{18}O ($\delta^{18}O$ around –107‰ and $\delta^{2}H$ around –423‰ V-SMOW). In addition, smaller volumes of test water and larger masses of rock were used. These modifications were necessary in order to obtain a modified test water composition after equilibration that is outside the standard analytical error of the mass-spectrometer. Obviously, solutions so much enriched in ^{2}H are difficult to analyse for $\delta^{2}H$ and certain memory effects cannot be excluded for some of the samples. In contrast, the oxygen isotope data are more reliable.

If successful, the diffusive isotope equilibration method delivers the stable isotope composition of pore water and the mass of pore water present in the connected pore space of the rock sample. The mass of pore water can be derived from the relation:

$$M_{PW} = \frac{M_{TW1} \cdot \left(C1^{\infty}_{TW1} - C1^{0}_{TW1}\right) + M_{TW2} \cdot \left(C2^{0}_{TW2} - C2^{\infty}_{TW2}\right)}{C2^{\infty}_{TW2} - C1^{\infty}_{TW1}} \qquad \text{(Eq. 3-2)}$$

where M = mass, $C\ 1,2$ = concentration of isotope tracer 1 and 2 in the test waters $TW1, 2$, PW = pore water, and the superscripts 0 and ∞ denote the tracer concentrations prior to and after equilibration of the test water with the pore water.

The stable isotope composition of the pore water is calculated from mass balance relationship of the experiments according to:

$$C_{PW} = \frac{\left(M_{TW1} \cdot C1^{\infty}_{TW1} \cdot C2^{\infty}_{TW2}\right) + \left(M_{TW1} \cdot C1^{0}_{TW1} \cdot C2^{\infty}_{TW2}\right) + \left(M_{TW2} \cdot C1^{\infty}_{TW1} \cdot C2^{\infty}_{TW2}\right) - \left(M_{TW2} \cdot C1^{\infty}_{TW1} \cdot C2^{0}_{TW2}\right)}{\left(M_{TW1} \cdot C1^{0}_{TW1}\right) + \left(M_{TW2} \cdot C2^{\infty}_{TW2}\right) - \left(M_{TW1} \cdot C1^{\infty}_{TW1}\right) - \left(M_{TW2} \cdot C2^{0}_{TW2}\right)} \qquad \text{(Eq. 3-3)}$$

where M = mass, C = isotope ratio, PW = pore water, TEW = test water, and the concentrations on the left side of the equation are prior to equilibration (t = 0), while the concentration on the right side is after equilibration is achieved (t = ∞) in the experiment. The two experiments deliver four equations of type (3-3) which are solved for the three unknown $\delta^{18}O_{PW}$, $\delta^{2}H_{PW}$ and M_{PW}.

The error of the calculated mass of pore water and pore water isotope composition is mainly sensitive to the ratio of pore water to test water used as can be shown by applying Gauss' law of error propagation (e.g. /Rübel 2000/). For the samples of borehole KFM02B, the error could be significantly reduced compared to the samples form earlier studies on material from boreholes KFM06A /Waber and Smellie 2005/ and KLX03 /Waber and Smellie 2006ab/. For borehole KFM02B the average error calculates to about ±1.2‰ for $\delta^{18}O$ and about ± 12‰ for $\delta^{2}H$.

3.2.3 Chemical composition of pore water

The chemical composition of pore water in the core material from borehole KFM02B was approached by out-diffusion experiments. These were performed on complete core samples of about 120 mm to 190 mm in length by immersion into ultra-pure water (Figure 3-1). To accelerate the out-diffusion, the vapour-tight PVC containers were placed into a water bath with a constant temperature of 45°C. The weight of the core sample, the experiment container, and the artificial test water used was measured before and after the experiment to ensure that no loss of test water occurred during the entire experiment. Weighing of the core before and after the experiment gives additional valuable information about the saturation state of the core at the beginning of the experiment.

At specific time intervals, initially a few days and later a few weeks, 0.5 mL of solution were sampled for the determination of the chloride concentration as a function of time. The small samples were analysed on a Metrohm 861 Compact ion-chromatograph for their anion content. A special set-up and method was developed to analyse low concentration of dissolved iodine, which was used as a tracer in the drilling fluid of the last about 15 m of the borehole. The analytical error of the anion determinations in the experiment solutions is about 5% based on multiple measurements of the standard solutions.

After equilibrium with respect to chloride was achieved, the core was removed from the container and the experiment solution was immediately analysed for pH and alkalinity (by titration). The remaining solution was split into different aliquots for chemical and isotopic analyses. Major cations and anions were analysed by ion-chromatography with a relative error of 5% based on multiple measurements of standard solutions. Dissolved silicon was analysed by photometry with a relative error of 5%.

Drilling fluid samples traced with iodine and taken at different times during drilling of the last 15 m of borehole KFM02B were analysed the same way and with the same analytical error.

The chloride concentration of the experiment solution can be converted to pore water concentrations using mass balance calculations given that steady-state conditions in the out-diffusion

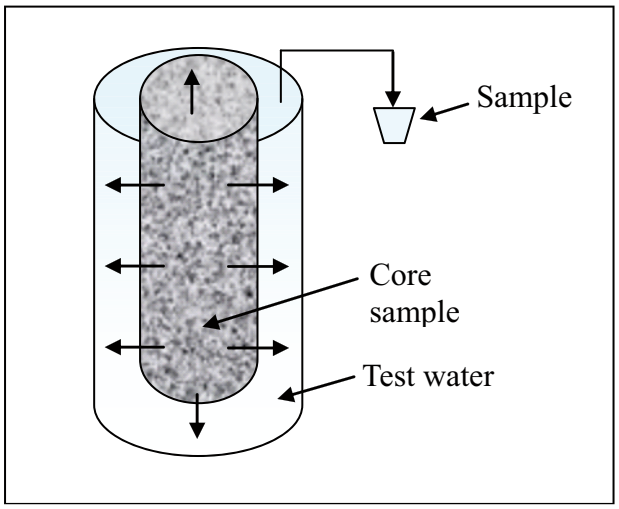

Figure 3-1. *Schematic diagram illustrating the out-diffusion experiments performed.*

experiment are attained. At steady-state conditions the chloride concentration in the connected porosity of the rock sample will be equal to that of the experiment solution. With knowledge of the mass of pore water in the rock sample, the chloride concentration of the pore water can be calculated according to:

$$C_{PW} = \frac{\left(M_{PW} + M_{TEWi} - \sum^{n} M_S\right) \cdot C_{equil,corrected} - (M_{TEWi} \cdot C_{TEWi}) + \sum^{n} M_S \cdot C_S}{M_{PW}} \quad \text{(Eq. 3-4)}$$

with:

$$C_{equil,corrected} = \frac{C_{TW_\infty} \cdot \left(M_{TWi} - \sum^{n} M_S\right)}{M_{TW_i}} \quad \text{(Eq. 3-5)}$$

where C = concentration, M = mass, n = number of samples and the subscripts PW = pore water, TEW = experiment solution, S = small-sized sample taken for chloride time-series, i = at beginning of experiment, and ∞ = at end of experiment.

The last term in Equation 3-4, $\Sigma M_S \cdot C_S$, describes the amount of chloride (and for the last four samples also of the drilling fluid tracer iodide) removed from the initial experiment solution by the chloride time-series samples. The final measured concentration of chloride in the experiment solution, $C_{TEW}\infty$, is corrected for the mass of solution removed by the chloride time-series samples from the initial mass of the experiment solution, M_{TEWi}, in order to obtain the chloride concentration in the experiment solution at steady state, $C_{equil,corrected}$ (Equation 3-5). A correction for chloride in the initial experiment solution ($M_{TEWi} \cdot C_{TEWi}$) is necessary if this solution is not entirely free of chloride.

It should be noted that the unit of pore water concentrations is given as mg/kg_{H2O} (and not mg/L) because it is derived on a mass basis rather than a volumetric basis. This is because the density of the pore water is not known beforehand. In reality and within the overall uncertainty band, the difference between mg/kg_{H2O} and mg/L becomes only important at an ionic strength of the calculated pore water above that of seawater (~0.7 M) corresponding to a total mineralisation of ~35 g/L.

3.3 Data handling

All data from this activity are stored in SKB's database Sicada, where they are traceable by Activity Plan number (AP PF 400-05-126). Only data in SKB's databases are accepted for further interpretation and modelling and the data presented in this report are regarded as copies of the original data. Data in the databases may be revised, if needed. Such revisions will not necessarily result in a revision of the P-report, although the normal procedure is that major data revisions entail a revision of the P-report. Minor data revisions are normally presented as supplements, available at *www.skb.se*.

3.4 Nonconformities

All activities have been performed according to the activity plan PF-400-05-126.

Exceptions include three samples where, during the diffusive isotope exchange, evaporation and/or condensation of test and pore water occurred on the walls of the vapour-tight container. The analysed isotope values of these three samples show a clear deterioration that can no longer be corrected for.

An integration of the pore water data with geological data (lithology, degree of alteration, fracture type and frequency etc) is limited for samples collected below 510 m borehole length because no on-site geological drillcore logging has been performed.

The major goal of the pore water investigations in borehole KFM02B, i.e. the detailed sampling of a continuous profile from a water-conducting zone into the intact rock matrix, could not be achieved because sampling in the field started at too great a distance from the demarcated highly transmissive zone.

4 Evaluation of pore water data

As mentioned previously, pore water residing in the low-permeability matrix of a rock body has to be characterised by indirect methods based on drillcore material because it cannot be sampled by conventional groundwater sampling techniques. Within the Forsmark and Laxemar Site Investigation programmes such attempts were undertaken for the first time in crystalline rocks by conducting various diffusion experiments with the core material retrieved from great depth in deep boreholes. Such determinations may be subjected to various types of induced perturbations, which need to be understood for the interpretation of so derived data with respect to *in situ* conditions. This required a rigorous control of the acquired data and supporting experiments in order to understand possible perturbation effects such as stress release, the drilling process, and sample de-saturation.

Most crucial in pore water investigations is the preservation of the original water-saturated state of the rock material that has not been affected by possible contamination by drilling fluid and air exposure. This requires a concerted logistic integration between the team on the drill site and in the laboratory, an immediate sample conditioning on site, and a rapid transport of the sample to the laboratory and subsequent sample preparation for the individual experiments. Yet, even if all these requirements are satisfied, some perturbation of the drillcore could have taken place already during drilling in the borehole. Such possible perturbations include the enlargement of the pore space of the rock by the drilling process and/or stress release, and mixing of the pore fluid with drilling fluid. The former would result in an overestimation of the water content and thus connected porosity of a drillcore sample, and the latter would result in either a dilution or enrichment of the pore water with conservative (and other) elements and isotopes.

To investigate the degree of such possible perturbation effects, sections of two newly drilled boreholes were drilled using chemically traced drilling fluid. The drillcore samples were subjected to exactly the same procedure as all other pore water samples including immediate conditioning on-site, fast shipping to the laboratory and performing out-diffusion experiments and all other necessary measurements just after arrival of the samples in the laboratory. One of these boreholes was drilled in the tunnel wall at the Äspö URL. Here, the effects of the drilling process were investigated as the rock is believed to be stress released after almost 20 years since excavation of the tunnel. The other one is the presently described borehole KFM02B at Forsmark, where spiked drilling fluid was used to drill the last 15 metres of the borehole down to 573.54 m borehole length. Here, it was hoped that the effects of stress release combined with the drilling process could be investigated.

The detailed results of these experiments and the sensitivity analyses of the data are given in /Waber et al. in prep./. The conclusion drawn from the study can be summarised as follows.

The drilling fluid contamination experiment conducted on a stress-released drillcore from the Äspö HRL revealed that:

- Modelling with a homogeneous pore diffusion coefficient (Dp) adequately describes the measured data of Cl^- and the I^- tracer.
- The chemically disturbed zone extends to a maximum of 0.1 mm into the drillcore which corresponds to about 0.66% of the total pore volume; this is consistent with a maximum contamination of <1% derived from tracer mass-balance considerations.
- The mechanically disturbed zone might be more heterogeneous and extend somewhat further into the drillcore (along grain boundaries), but the total affected pore volume is that derived from the chemically disturbed zone.
- No measurable ingress of drilling fluid, i.e. no contamination, has occurred in the drilling disturbed zone (DDZ) of the drillcore within a contact time of 2 hours.

The drilling-fluid contamination experiment conducted on drillcores from about 560 m depth in borehole KFM02B at Forsmark revealed that:

- Modelling with a homogenous Dp cannot adequately describe the measured data of Cl^- and the I^- tracer.
- The extent of the mechanically disturbed zone, i.e. expected heterogeneous diffusion properties, extends within the outermost 6 mm of the drillcore.
- The chemically disturbed zone extends to a maximum of 0.3 mm into the drillcore based on mass balance considerations of the tracer concentration, and 0.15 mm to 0.2 mm into the drillcore based on comparing the observed artificial (I^-) and natural (Cl^-) tracer data. This corresponds to a maximum of 2.4% of the total pore volume being affected by the drilling-fluid contamination.
- The maximum contamination of the pore water Cl^- concentration is about 8%.

Based on these results it can be concluded that the Cl^- contamination by drilling fluid of the drillcores from borehole KFM02B at Forsmark is being less than 10% and, therefore, is within the uncertainty band of the pore water determinations. The uncertainty of the indirect pore water investigations is thus essentially given by the measurement of the water-content and connected porosity, respectively.

5 Petrophysical rock properties

The petrophysical properties determined on the drillcore samples from borehole KFM02B include the water content derived by different methods, the bulk wet density, and the water-loss porosity. All water-content measurements were conducted on originally saturated samples.

5.1 Water content

5.1.1 Gravimetric water content

The wet rock mass of small-sized samples used for gravimetric water content determinations ranged between about 90–300 g for samples specifically assigned for these measurements, and between about 180–380 g for the samples previously used in the isotope exchange experiments. The water content of 37 out of 39 drillcore samples varies between 0.12–0.26 wt.% with an average 0.19 ± 0.06 wt.% (Table 5-1). Sample 2B-2 (171.83 m) and 2B-13 (498.84 m) have higher values of 0.42 wt.% and 0.34 wt.%, respectively, and both are associated with highly tectonised and altered zones with a high fracture frequency (cf. Figure 2-2).

The wet rock mass of large-sized core samples used for out-diffusion experiments and subsequently for gravimetric water content determinations, ranged between about 580–1,000 g (Table 5-2). The rapid core preservation on the drill site and the sample conditioning in the laboratory within about 24 hours after core recovery were successful and indispensable for the preservation of the original saturated state of the drillcore samples. The difference of less than 1‰ in weight before and after the out-diffusion experiment, i.e. after more than 3 months of water immersion of the samples, shows that the samples were originally saturated (Figure 5-1). For the large-sized samples the water content of 37 out of 39 drillcore samples varies between 0.14–0.33 wt.% with an average 0.21 ± 0.04 wt.% (Table 5-1). As for the small-scaled samples, again samples 2B-2 (171.83 m) and 2B-13 (498.84 m) have higher values of 0.27 wt.% and 0.34 wt.%, respectively, compared to all other large-sized drillcore samples. Whereas for sample 2B-13 (including three sub-samples) the water content of the small-sized and the large-sized sample are identical, those for sample 2B-2 are greatly different (Table 5-1). Based on petrographic investigations of sample 2B this must be attributed to sample heterogeneity, i.e. the occurrence of closed hair fissures in the small-sized samples.

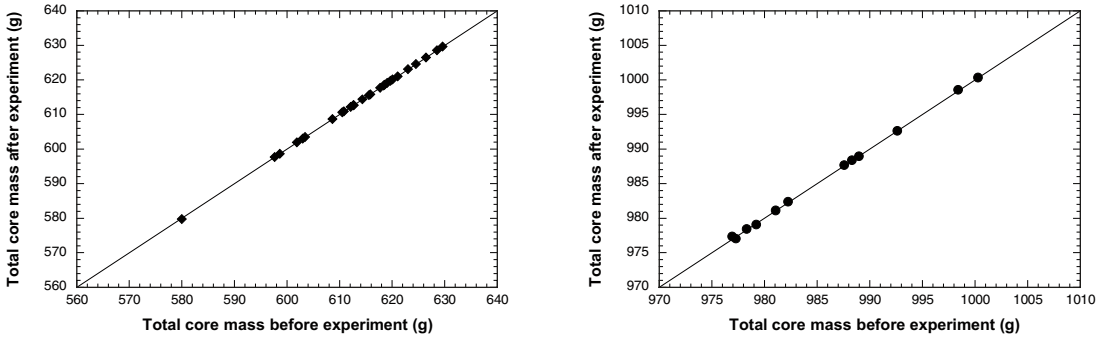

Figure 5-1. *Borehole KFM02B: Wet rock mass of the 39 drillcore samples used for out-diffusion experiments before and after the experiment, i.e. before and after immersion in test water over a 3 months period. The identical weights indicate preservation of the originally saturated state of the samples upon arrival in the laboratory (measurement error of 10% is within the size of the symbols; left: samples of about 12 cm in length, right: samples of about 19 cm in length).*

In general, the water content obtained for the large-sized samples is slightly higher than that of the small-sized samples (Figure 5-2). This is attributed to the greater risk of partial desaturation during sample preparation of small-scaled samples. Also, the ratio of newly created surfaces to the bulk mass of the sample, and thus the effect of evaporation, is larger for such small-sized samples compared to the large-size samples used for out-diffusion experiments.

The water contents of both types of samples display an identical behaviour in that there is no correlation with increasing depth (Figure 5-2). This argues against a measurable contamination of the samples induced by stress release and drilling fluid contamination. This is also confirmed by the results of the samples drilled with traced drilling fluid (see Chapter 4). In turn, a correlation is established with the degree of alteration and brittle deformation of the rock. Elevated water contents are clearly related to stronger deformed zones of higher transmissivity as, for example, observed around zones of higher fracture frequency between about 400–520 m and again at 560 m borehole length.

5.1.2 Water content by diffusive isotope exchange

The water content derived by the diffusive isotope exchange method varies for all samples between 0.13–0.36 wt.% with an average of 0.19 ± 0.05 wt.% (Table 5-1). For most samples, the water content derived by this method is slightly lower compared to that derived by gravimetric methods (Figure 5-2). In only three samples does the water content derived by isotope exchange exceed the experimental and analytical uncertainty compared to the gravimetric water contents. This contrasts to some degree with previous experience from the Forsmark site /cf. Waber and Smellie 2005, 2007/, although this might be explained by the different mineralogy of the rocks in borehole KFM02B compared to that in previous boreholes drilled in the footwall to the north. In borehole KFM02B the rocks seem more leucocratic and have less sheet silicates which might reduce the exchange with bound water on the surface of such minerals. This has been proposed to explain the commonly slightly higher water contents derived by the diffusive isotope exchange method compared to gravimetrically derived approach (e.g. /Pearson et al. 2003/).

In spite of the slight absolute difference in water contents derived by the two methods, there is no difference between the obtained data if plotted against depth (Figure 5-3). The same correlation between water derived by the diffusive isotope exchange method and stronger deformed zones of higher transmissivity is observed, whereas no trend is established as a function of depth. Therefore, all three data sets of water content argue against a measurable influence of stress release and any associated induced drilling fluid contamination.

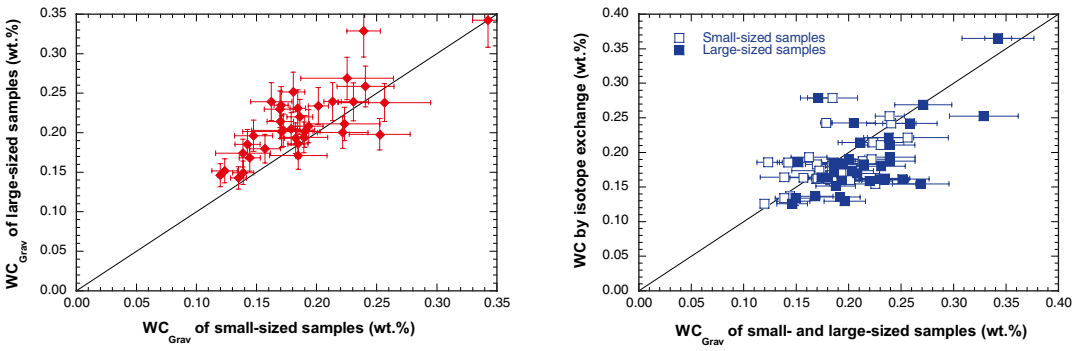

Figure 5-2. *Borehole KFM02B: Comparison of gravimetric water determined on small-sized and large-sized samples (left) and the water content derived by diffusive isotope exchange (right; see Table 5-1 for explanation of the error bars).*

Table 5-1. KFM02B borehole: Gravimetric water content by drying at 105°C (WC_{Grav}) and diffusive isotope exchange (WC_{IsoEx}) of drillcore samples.

Laboratory sample No	Borehole length	Small-sized samples			Large-sized samples		Isotope exchange	
		No of samples	WC_{Grav} average	error 1 σ	Mass	WC_{Grav} [1]	WC_{IsoEx} average	error [2]
	(m)		(wt.%)	(wt.%)	(g)	(wt.%)	(vol.%)	(vol.%)
KFM02B-1	158.91	1	0.252	0.025	579.935	0.198	[3]	
KFM02B-2	171.83	3	0.423	0.020	979.235	0.271	0.269	0.002
KFM02B-3	210.64	3	0.184	0.008	992.617	0.186	0.172	0.002
KFM02B-4	287.16	3	0.179	0.005	988.984	0.205	0.243	0.002
KFM02B-5	393.29	3	0.213	0.007	612.652	0.239	0.188	0.002
KFM02B-6	430.74	3	0.135	0.007	615.826	0.143	[3]	
KFM02B-7	441.45	3	0.182	0.009	629.623	0.193	0.160	0.002
KFM02B-8	448.06	3	0.222	0.021	1000.288	0.200	0.190	0.002
KFM02B-9	459.84	3	0.120	0.002	988.312	0.146	0.126	0.002
KFM02B-10	474.07	3	0.189	0.020	618.420	0.194	0.184	0.003
KFM02B-11	478.89	3	0.147	0.016	998.407	0.196	0.129	0.002
KFM02B-12	490.46	3	0.225	0.039	621.058	0.269	0.154	0.002
KFM02B-13	498.84	3	0.343	0.013	619.712	0.342	0.365	0.003
KFM02B-14	509.81	3	0.241	0.024	618.585	0.258	0.242	0.002
KFM02B-15	512.57	3	0.223	0.029	626.453	0.211	0.214	0.002
KFM02B-16	512.96	3	0.123	0.011	610.801	0.152	0.186	0.003
KFM02B-17	513.34	3	0.144	0.009	982.236	0.168	0.137	0.002
KFM02B-18	513.68	3	0.170	0.011	624.518	0.214	0.183	0.002
KFM02B-19	514.04	3	0.157	0.013	602.977	0.180	0.163	0.002
KFM02B-20	514.47	3	0.171	0.032	597.663	0.201	[3]	
KFM02B-21	514.84	3	0.186	0.011	978.324	0.220	0.158	0.002
KFM02B-22	515.19	3	0.162	0.017	598.639	0.239	0.193	0.002
KFM02B-23	515.54	3	0.172	0.026	608.625	0.203	0.174	0.003
KFM02B-24	515.85	3	0.141	0.011	620.086	0.192	0.135	0.003
KFM02B-25	516.12	3	0.152	0.014	619.087	0.188	0.151	0.002
KFM02B-26	516.42	3	0.142	0.010	614.313	0.186	0.186	0.002
KFM02B-27	516.72	3	0.201	0.008	612.645	0.234	0.160	0.002
KFM02B-28	517.03	3	0.184	0.006	628.536	0.231	0.180	0.002
KFM02B-29	517.34	3	0.180	0.010	623.052	0.251	0.162	0.002
KFM02B-30	519.54	3	0.139	0.023	601.863	0.174	0.164	0.002
KFM02B-31	522.11	3	0.139	0.009	612.115	0.149	0.134	0.003
KFM02B-32	522.39	3	0.185	0.024	610.514	0.171	0.279	0.002
KFM02B-33	527.55	3	0.169	0.013	603.422	0.230	0.162	0.002
KFM02B-34	532.44	3	0.190	0.007	617.691	0.202	[3]	
KFM02B-39	559.83	3	0.170	0.006	615.578	0.235	0.163	0.003
KFM02B-40	562.47	3	0.231	0.013	981.065	0.239	0.211	0.003
KFM02B-41	565.29	3	0.256	0.039	977.289	0.238	0.222	0.002
KFM02B-42	569.35	3	0.239	0.014	976.949	0.329	0.253	0.003
KFM02B-43	573.65	3	0.193	0.012	987.576	0.208	0.170	0.003

[1] – = Error assumed to be 10%, [2] Error calculated with Gauss' law of error propagation.
[3] – = Experiment not performed or experiment failed.
Borehole length values represent preliminary borehole data when sampled in the field.

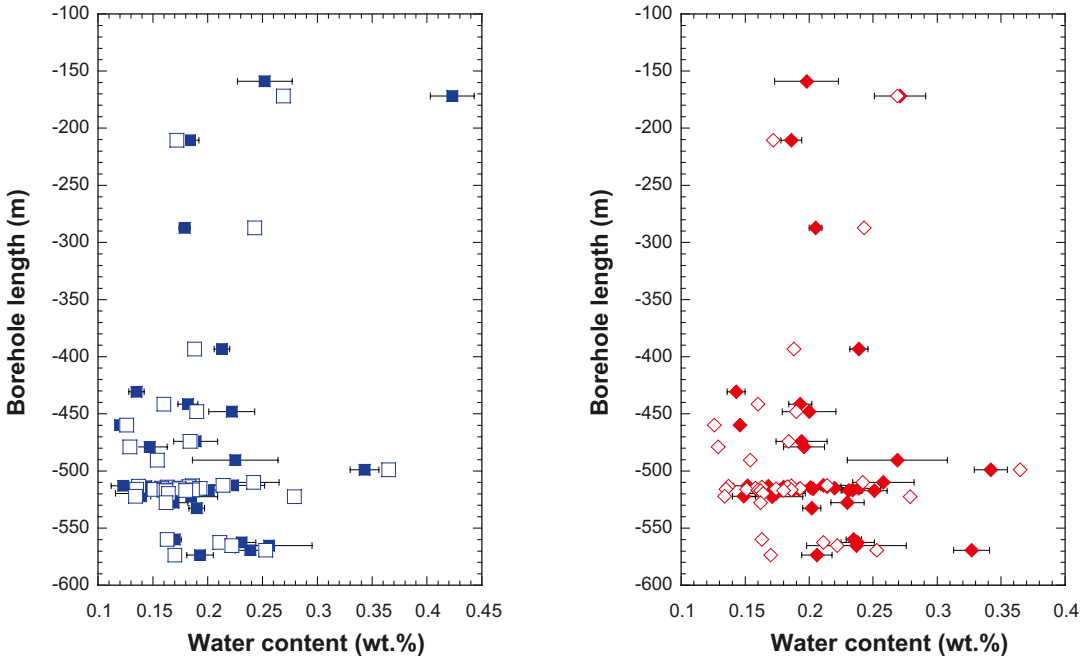

Figure 5-3. *Borehole KFM02B: Gravimetric water content derived by drying at 105°C of small-scaled samples (closed symbols, left) and large-scale samples (closed symbols, right) compared to water content derived by diffusive isotope exchange (open symbols).*

5.2 Bulk density

The bulk density was derived from the wet mass and the volume of the large-sized drillcore samples used for the out-diffusion experiments. Although the volumetric measurement might not be as accurate as other techniques, the large size and the well-shaped drillcores allowed reasonable estimates of the bulk wet density. It varies between 2.61–2.67 g/cm^3 with an average of 2.64 ± 0.01 g/cm^3 (Table 5-2). Such bulk density is concurring with the mineralogy of the rock samples and compares well with bulk density values derived by other methods for the predominantly metagranite to metagranodiorite type rocks (e.g. /Liedberg 2006/).

5.3 Water-loss porosity

As will be shown in Chapter 6, the salinity of the pore water is far below that of sea water in all samples. Therefore, the assumption of a density for the pore water of one is justified and the calculation of the water-loss porosity from the water content according to Equation 3-1 becomes a simple scaling with the rock density. Because the rock density of all samples displays only a small variation, all dependencies and trends described for the water content also account for the water-loss porosity, especially those versus depth (Figure 5-4).

For the small-sized samples, the water-loss porosity of 37 out of 39 drillcore samples varies from 0.32–0.67 vol.% with an average 0.48 ± 0.10 vol.% (Table 5-2). Exceptions are again samples 2B-2 with 1.11 vol.% and sample 2B-13 with 0.90 vol.% of water-loss porosity. For the large-sized samples, it varies from 0.38–0.86 vol.% with an average 0.55 ± 0.10 vol.% and sample 2B-2 and 2B-13 having a water-loss porosity of 0.71 vol.% and 0.90 vol.%, respectively (Table 5-2). Finally the water-loss porosity derived from diffusive isotope exchange varies from 0.33–0.96 vol.% for all samples with an average of 0.50 ± 0.13 vol.%.

Table 5-2. KFM02B borehole: Water-loss porosity (WL-P) determined by gravimetry and isotope exchange and bulk density of drillcore samples.

Laboratory sample No	Borehole length	Small-sized samples			Large-sized samples		Isotope exchange	
		No of samples	$WL\text{-}P_{Grav}$ average	error 1 σ	Bulk Density [1]	$WL\text{-}P_{Grav}$ [2]	$WL\text{-}P_{IsoEx}$ average	error [3]
	(m)		(wt.%)	(wt.%)	(g/cm³)	(vol.%)	(vol.%)	(vol.%)
KFM02B-1	158.91	1	0.66	0.03	2.65	0.52	[4]	
KFM02B-2	171.83	3	1.11	0.05	2.64	0.71	0.71	0.002
KFM02B-3	210.64	3	0.49	0.02	2.65	0.49	0.46	0.002
KFM02B-4	287.16	3	0.47	0.01	2.64	0.54	0.64	0.002
KFM02B-5	393.29	3	0.56	0.02	2.62	0.63	0.49	0.002
KFM02B-6	430.74	3	0.36	0.02	2.65	0.38	[4]	
KFM02B-7	441.45	3	0.48	0.02	2.65	0.51	0.42	0.002
KFM02B-8	448.06	3	0.58	0.06	2.64	0.53	0.50	0.002
KFM02B-9	459.84	3	0.32	0.01	2.65	0.39	0.33	0.002
KFM02B-10	474.07	3	0.50	0.05	2.65	0.51	0.49	0.003
KFM02B-11	478.89	3	0.39	0.04	2.64	0.52	0.34	0.002
KFM02B-12	490.46	3	0.59	0.10	2.67	0.71	0.41	0.002
KFM02B-13	498.84	3	0.90	0.03	2.63	0.90	0.96	0.003
KFM02B-14	509.81	3	0.63	0.06	2.64	0.68	0.64	0.002
KFM02B-15	512.57	3	0.59	0.08	2.65	0.56	0.57	0.002
KFM02B-16	512.96	3	0.33	0.03	2.63	0.40	0.49	0.003
KFM02B-17	513.34	3	0.38	0.02	2.64	0.44	0.36	0.002
KFM02B-18	513.68	3	0.45	0.03	2.62	0.56	0.48	0.002
KFM02B-19	514.04	3	0.41	0.03	2.64	0.47	0.43	0.002
KFM02B-20	514.47	3	0.45	0.08	2.64	0.53	[4]	
KFM02B-21	514.84	3	0.49	0.03	2.64	0.58	0.42	0.002
KFM02B-22	515.19	3	0.43	0.04	2.64	0.63	0.51	0.002
KFM02B-23	515.54	3	0.45	0.07	2.64	0.53	0.46	0.003
KFM02B-24	515.85	3	0.37	0.03	2.65	0.50	0.36	0.003
KFM02B-25	516.12	3	0.40	0.04	2.63	0.49	0.40	0.002
KFM02B-26	516.42	3	0.38	0.03	2.65	0.49	0.49	0.002
KFM02B-27	516.72	3	0.53	0.02	2.65	0.61	0.42	0.002
KFM02B-28	517.03	3	0.48	0.02	2.64	0.61	0.48	0.002
KFM02B-29	517.34	3	0.47	0.03	2.64	0.66	0.43	0.002
KFM02B-30	519.54	3	0.37	0.06	2.64	0.46	0.43	0.002
KFM02B-31	522.11	3	0.37	0.02	2.65	0.39	0.35	0.003
KFM02B-32	522.39	3	0.49	0.06	2.64	0.45	0.74	0.002
KFM02B-33	527.55	3	0.45	0.03	2.64	0.60	0.43	0.002
KFM02B-34	532.44	3	0.50	0.02	2.64	0.53	[4]	
KFM02B-39	559.83	3	0.45	0.02	2.63	0.62	0.43	0.003
KFM02B-40	562.47	3	0.61	0.03	2.64	0.63	0.56	0.003
KFM02B-41	565.29	3	0.67	0.10	2.63	0.62	0.58	0.002
KFM02B-42	569.35	3	0.63	0.04	2.61	0.85	0.66	0.003
KFM02B-43	573.65	3	0.51	0.03	2.64	0.55	0.45	0.003

[1] Determined from volume and mass, [2] Error assumed to be 10%, [3] Calculated with Gauss' law of error propagation.
[4] Experiment not performed or experiment failed.
Borehole length values represent preliminary borehole data when sampled in the field.

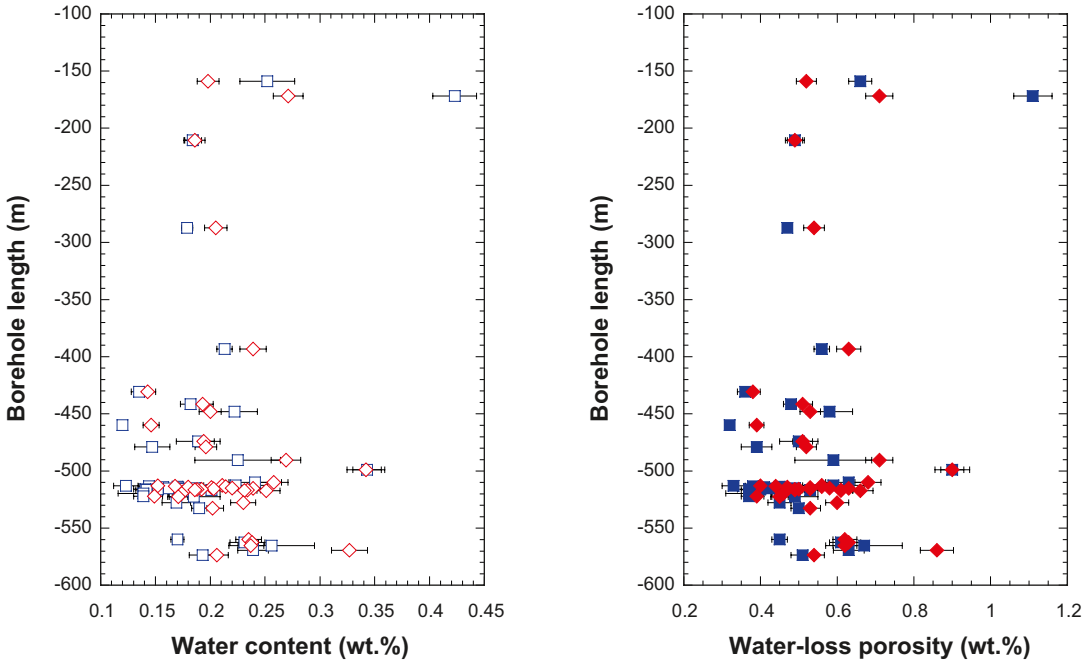

Figure 5-4. *Borehole KFM02B: Gravimetric water content (105°C; left) and water-loss porosity (right) of small-sized samples (blue squares) and large-sized out-diffusion experiment samples (red diamonds).*

6 Pore water composition

6.1 Out-diffusion experiments

Out-diffusion experiments have been performed on 39 core samples from borehole KFM02B. From 150 m to 450 m borehole length, the samples were collected on-site from fracture-free rock portions with the most proximate open and/or closed fracture being at least 5 m away if possible. At greater depth, samples were collected at smaller intervals in order to include the demarcated water-conducting zones ZFMA2/ZFMF1 which had been predicted to be intercepted between 423 m (upper intercept) and 503 m (lower intercept). Initially, a highly conductive zone with a transmissivity of more than 10^{-5} m^2/s was encountered at about 471 m and a second one of similar transmissivity at about 501 m depth /Väisäsvaara and Pöllänen 2007/. However, because the predicted water-conducting zone was not immediately recognised at this greater depth during drilling, continuous sampling of 5 m of fresh core material away from the water-conducting zone did not start until the next core length was retrieved, i.e. at about 512 m borehole length. Below 517 m the intervals were again increased to 2 m and finally to about 5 m down to the end of the borehole.

The last five samples collected between 559.83–573.65 m borehole length (samples 2B-39 to 2B-43) were drilled using a drilling fluid that was spiked with 1 g of iodide. These samples were used to investigate the effects of possible drilling fluid contamination of the core sections induced by stress release and the drilling process. The time-series solutions and the final experiment solution of these samples were investigated for dissolved I^- in addition to Cl^-.

For the continuously sampled profile away from a water-conducting zone the distance between individual samples was optimised. This resulted in 27 samples comprising about 12 cm long intact core pieces used for the out-diffusion experiments, whereas about 19 cm were used for the remaining samples. In all experiments the weight ratio of test water to rock was maintained between about 0.104–0.139 and the experiment temperature was 45°C (Table 6-1).

6.1.1 Equilibrium control in the out-diffusion experiment

The monitoring of steady-state conditions in the out-diffusion experiments was performed with extracting small-sized samples of 0.5 mL at regular intervals and analysed for their anion concentration. Equilibrium conditions with respect to chloride concentrations in the remnant solution in the pore volume of the rock and the test water in the sample container is attained when the chloride time-series concentrations reach a plateau, i.e. when they remain constant. With respect to the out-diffusion of chloride, equilibrium conditions have been attained in the experiments after about 50 to 60 days independent of the sample mass, porosity or depth of sampling (Figure 6-1). To allow a complete equilibration, the experiment time was between 112–116 days for all samples and based on previous experience.

6.1.2 Chemical composition of experiment solutions

The chemical composition of the supernatant solutions after termination of the out-diffusion experiments is given in Table 6-1. The quality of the chemical analyses is excellent as can be seen from the charge balance between dissolved cations and anions, which is better than ± 5% for all samples except one (2B-1) and averages at 2.5 ± 1.6%.

The pH of the experiment solutions varied between 6.97 and 7.44 and the total mineralisation ranged from 162 mg/L to 366 mg/L. It should be noted that the total mineralisation obtained for the experiment solutions is dependent on the water content of the sample and the water/rock ratio used in the experiment (Table 5-1) and does not directly reflect differences in pore water salinity.

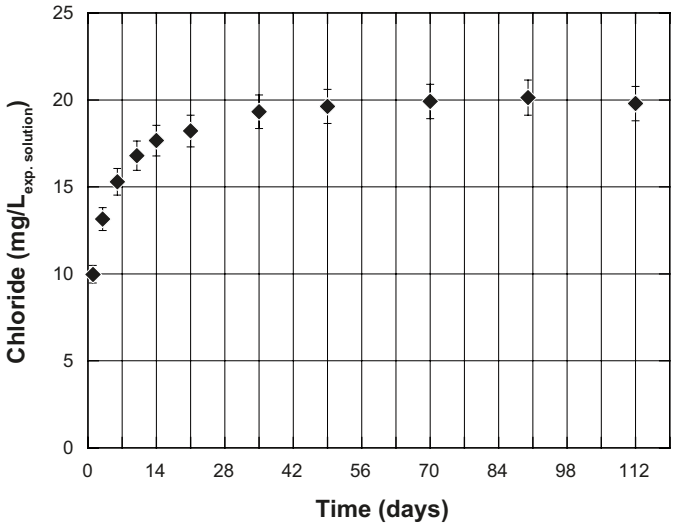

Figure 6-1. *Borehole KFM02B: Example of chloride time-series displaying that steady-state conditions in the out-diffusion experiments were achieved after about 50 days (sample KFM02B-26, borehole length = 516.42 m, ΦWL = 0.49 vol.%).*

Furthermore, mineral dissolution that occurs during the experiment obviously affects to a certain degree the concentrations of reactive compounds, pH and total mineralisation so that these are not representative for *in situ* pore water. Major reactions that affect measured elemental concentrations in the experiment solutions involve the dissolution of plagioclase (Ca, Na), K-feldspar (K), biotite (K, Mg), muscovite (K), chlorite (Mg) and possibly fluorite (F), pyrite (SO_4) and calcite (Ca, CO_3). The dissolution of Al-silicate minerals consumes carbonic acid present in the initial test water and will also change the total alkalinity. Because the general rock mineralogy is rather constant for all investigated samples, mineral dissolution during the experiments is expected to be similarly uniform.

By applying geochemical model calculations including mineral dissolution kinetics, the contribution from mineral dissolution during the out-diffusion experiment can be estimated. Such calculations have been performed using the geochemical code PHREEQC /Parkhurst and Appelo 1999 v.2.15, 2008/ and the kinetic rate laws given in the WATEQ4F database attached to this code (for details see /Waber et al. in prep./). As suggested by these calculations, the weathering reactions during the out-diffusion experiment do not significantly alter the general chemical type of the experiment solutions, except for dissolved carbonate. The latter is due to the partial open system conditions under which the experiments were performed, whereas the theoretical simulation reflects closed system conditions. With this exception, the chemical type determined on the basis of the experiment solution is qualitatively acceptable as being that of the *in situ* pore water.

Furthermore, the calculations suggest that the contribution of cations to the experiment solution by weathering reactions during the experiment time of around 110 days is less than about $10^{-4.5}$ mol/L, i.e. less than about 0.03 mmol/L (Figure 6-2). For Mg^{2+}, for instance, this converts to a contribution from weathering of less than about 0.7 mg/L during the experiment. This value might well be overestimated because in the calculations a larger fraction of biotite was assumed, as it is actually present in the rocks of borehole KFM02B. In any case, it suggests that in experiment solutions where Mg^{2+} is present in concentrations of more than 0.8 mg/L, a significant fraction of the Mg^{2+} comes from the pore water itself. This allows the resolution of pore waters with Mg^{2+} contents that are below about 20 mg/L and above 100 mg/L, the latter being indicative for a Littorina and/or Baltic Sea component in the pore water.

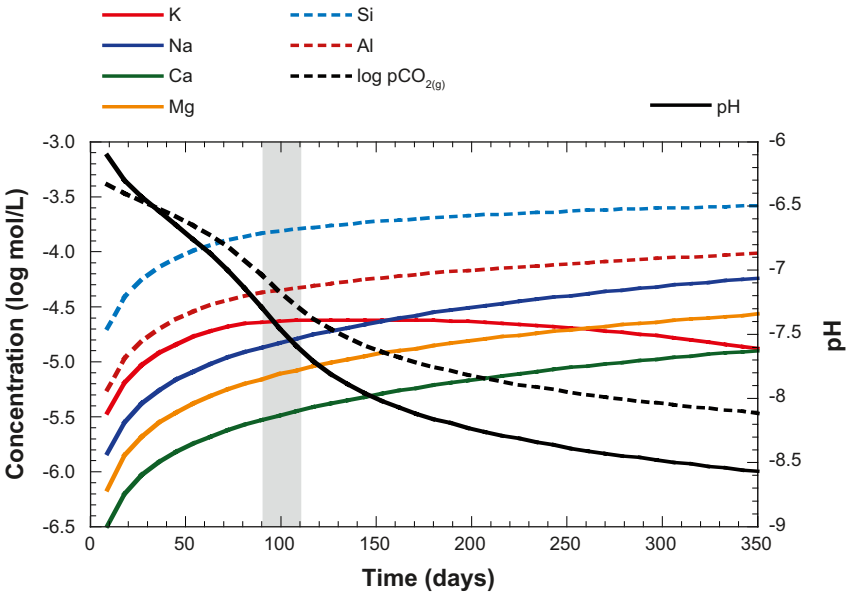

Figure 6-2. *Calculated cation concentrations, $pCO_{2(g)}$, and pH during kinetic weathering of a granite at 45°C. The shaded area gives the experiment time of the out-diffusion experiment conducted with the drill core material from borehole KFM02B. Note the low concentration of all cations, but especially Mg, even after one year of hypothetical experiment time.*

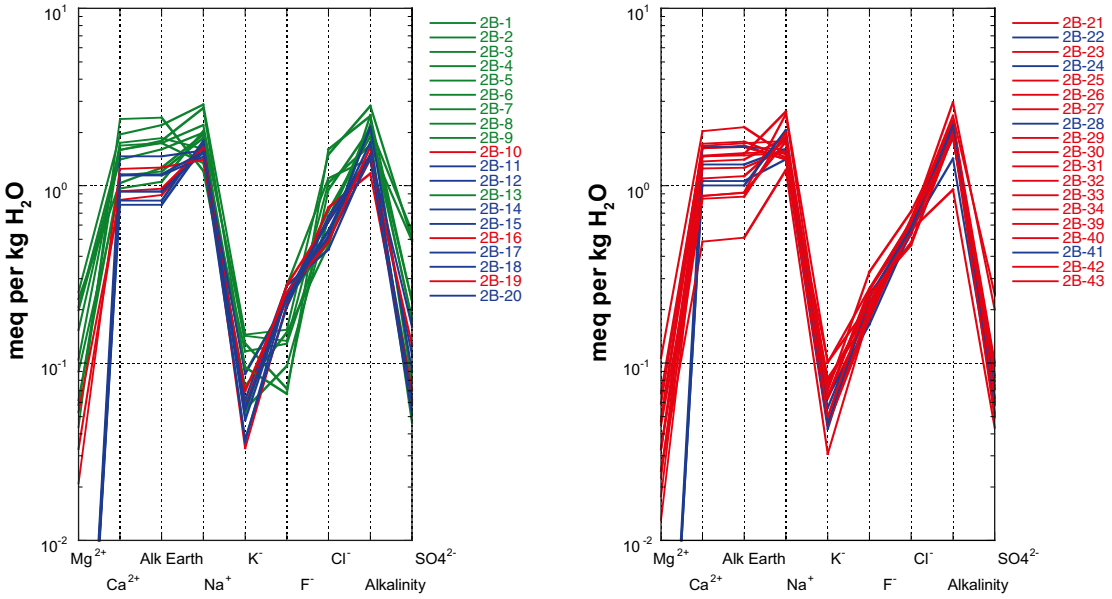

Figure 6-3. *Borehole KFM02B: Schoeller diagram of experiment solutions from the drillcore samples 2B-1 to 2B-20 (left) and 2B-21 to 2B-43 (right). Note the larger variation in chemical type at shallow depths (small sample numbers) compared to the deformation zone ZFMF1 and its near vicinity (sample numbers >14; chemical types: green = Ca-Na-HCO_3, blue = Na-Ca-HCO_3, red = Na-Ca-HCO_3-Cl).*

The chemical character of the experiment solutions is fairly similar and represents a Na-Ca-HCO_3-Cl type for most samples (Figure 6-3). Compositional differences are restricted to the ratios of alkaline earth elements (Ca^{2+}, Mg^{2+}, Sr^{2+}) to the total alkalinity, Na^- and Cl^-. Minor variations in mineralisation and ion-ion ratios are somewhat more expressed at shallow depth in the borehole, whereas the samples collected from the near-vicinity of water-conducting zones at greater depth appear to be more homogeneous. Although present in low concentrations, significant differences in Mg^{2+} are observed (often associated with K^+ concentrations) at intermediate depths (Figure 6-3). To what degree bicarbonate (HCO_3^-) forms part of the chemical type of the *in situ* pore water is currently difficult to judge as outlined below.

The amount of dissolved carbonate in the experiment solution was determined by alkalinity titration and expressed as bicarbonate (HCO_3^-). The initial test solution was deionised water with a negligible amount of dissolved carbon. Therefore, the measured total alkalinity and the calculated total carbon concentration in the solutions at the end of the experiments must essentially come from the pore water and/or carbon-providing mineral reactions during the experiment. In spite of the partial open system conditions under which the experiments were performed, a large contamination induced by the experiment set-up can be excluded because such contamination cannot surpass the carbon concentration in equilibrium with atmospheric CO_2. The only exception would be if large amounts of carbonate minerals would be present in the rock, but this is not the case. Geochemical model calculations show that at the measured conditions the experiment solutions are undersaturated with respect to calcite at corresponding high partial pressures of CO_2 (log pCO_2 of around –2). Together with the low abundance of carbonate minerals in the rock, this suggests that mineral carbonate is only a minor source of carbon in this system. Thus, most of the dissolved carbon appears to originate from the pore water where it presumably occurs mainly in the oxidised state (HCO_3^-, CO_3^{-2}). However, the existence of dissolved reduced carbon (e.g. CH_4) as, for example, observed in groundwaters sampled from borehole KFM02B, cannot be excluded. The presence of substantial amounts of dissolved gas in the pore water was supported by the observation of an increase in pressure in the experiment devices during the first days, suggesting that degassing of pressurised gas such as dissolved CO_2 and/or CH_4 occurred in the initial stages of the experiment. Besides the carbonate dissolution reactions, this inhibits the direct comparison of the measured carbonate system parameters to those present under *in situ* conditions.

Table 6-1. Chemical composition of solutions from out-diffusion experiments at steady-state conditions.

Out-diffusion experiment solution	Units	KFM02B-1	KFM02B-2	KFM02B-3	KFM02B-4	KFM02B-5	KFM02B-6	KFM02B--7	KFM02B-8
SAMPLE DESCRIPTION									
Borehole length	m	158.91	171.83	210.64	287.16	393.29	430.74	441.45	448.06
Rock type									
Water-rock ratio		0.139	0.113	0.114	0.109	0.110	0.111	0.109	0.104
Experiment temperature	ºC	45	45	45	45	45	45	45	45
Experiment time	days	115	115	115	115	115	115	115	115
MISC. PROPERTIES									
Chemical type		Ca-Na-HCO_3-Cl	Na-Ca-HCO_3-Cl	Na-Ca-HCO_3-Cl	Ca-Na-HCO_3-Cl	Ca-Na-HCO_3-Cl	Na-Ca-HCO_3-Cl	Na-Ca-HCO_3-Cl	Na-Ca-HCO_3-Cl
pH (lab)	-log(H+)	7.28	7.37	7.41	7.08	7.17	6.97	6.98	7.26
Sample temperature	ºC	20	20	20	20	20	20	20	20
CATIONS									
Sodium (Na^+)	mg/L	27.9	46.8	42.9	30.9	37.1	45.8	50.6	66.1
Potassium (K^+)	mg/L	2.9	2.3	3.5	4.6	2.2	5.6	5.0	5.7
Magnesium (Mg^{+2})	mg/L	0.5	1.1	0.8	0.7	1.3	2.4	1.9	3.1
Calcium (Ca^{+2})	mg/L	47.7	19.3	22.9	33.9	35.1	28.2	32.0	39.1
Strontium (Sr^{+2})	mg/L	<0.5	<0.5	<0.5	<0.5	<0.5	<0.5	<0.5	<0.5
ANIONS									
Fluoride (F^-)	mg/L	2.8	4.4	4.3	2.4	1.8	2.5	1.4	2.9
Chloride (Cl^-)	mg/L	16.3	25.7	17.0	23.0	23.2	37.0	33.7	53.2
Bromide (Br^-)	mg/L	<0.5	<0.5	<0.5	<0.5	<0.5	<0.5	<0.5	<0.5
Sulphate (SO_4^{-2})	mg/L	3.7	2.2	8.3	8.6	10.8	23.6	26.5	24.1
Nitrate (NO_3^-)	mg/L	4.2	1.7	<0.5	<0.5	<0.5	0.8	<0.5	<0.5
Total alkalinity	meq/L	2.51	1.90	2.22	2.04	2.16	1.70	2.11	2.82
NEUTRAL SPECIES									
Aluminium (Al tot)	mg/L	0.064	0.046	0.052	0.054	0.045	0.060	0.033	0.042
Silica (Si tot)	mg/L			15.1	9.7	8.2	11.6	5.7	14.2
CALC. PARAMETERS									
Total dissolved solids	mg/L	255	217	234	228	242	246	280	366
Charge balance	%	6.39%	3.61%	0.76%	3.30%	5.84%	5.00%	5.05%	2.34%

Table 6-1. (page 2 of 5).

Out-diffusion experiment solution	Units	KFM02B-9	KFM02B-10	KFM02B-11	KFM02B-12	KFM02B-13	KFM02B-14	KFM02B--15	KFM02B-16
SAMPLE DESCRIPTION									
Borehole length	m	459.84	474.07	478.89	490.46	498.84	509.81	512.57	512.96
Rock type									
Water-rock ratio		0.107	0.108	0.106	0.111	0.111	0.115	0.115	0.116
Experiment temperature	ºC	45	45	45	45	45	45	45	45
Experiment time	days	115	112	112	112	112	112	112	112
MISC. PROPERTIES									
Chemical type		Na-Ca-HCO_3-Cl	Na-Ca-HCO_3-Cl	Na-Ca-HCO3	Na-Ca-HCO3	Na-Ca-HCO_3-Cl	Na-Ca-HCO_3-Cl	Na-Ca-HCO_3-Cl	Na-Ca-HCO_3-Cl
pH (lab)	-log(H+)	7.32	7.29	7.33	7.22	7.38	7.19	7.29	7.27
Sample temperature	ºC	20	20	20	20	20	20	20	20
CATIONS									
Sodium (Na^+)	mg/L	44.8	38.4	36.3	39.0	63.1	41.2	38.3	37.7
Potassium (K^+)	mg/L	2.0	1.3	3.4	2.4	3.7	1.4	1.9	2.2
Magnesium (Mg^{+2})	mg/L	2.8	0.6	<0.3	<0.3	2.5	<0.3	<0.3	0.4
Calcium (Ca^{+2})	mg/L	20.7	16.7	29.4	18.6	31.8	16.5	15.6	18.6
Strontium (Sr^{+2})	mg/L	<0.5	<0.5	<0.5	<0.5	<0.5	<0.5	<0.5	<0.5
ANIONS									
Fluoride (F^-)	mg/L	5.2	4.1	4.3	5.2	1.3	4.7	4.7	5.2
Chloride (Cl^-)	mg/L	39.1	26.8	18.4	15.5	56.8	19.8	17.7	22.7
Bromide (Br^-)	mg/L	<0.5	<0.5	<0.5	<0.5	<0.5	<0.5	<0.5	<0.5
Sulphate (SO_4^{-2})	mg/L	3.4	3.4	4.4	7.7	10.7	5.4	2.5	6.1
Nitrate (NO_3^-)	mg/L	9.3	7.6	<0.5	8.1	11.7	3.2	10.6	5.7
Total alkalinity	meq/L	1.42	1.17	2.15	1.51	2.48	1.50	1.41	1.41
NEUTRAL SPECIES									
Aluminium (Al tot)	mg/L	0.083	0.071	0.089	0.077	0.048	0.070	0.100	0.109
Silica (Si)	mg/L	10.6	5.8	11.4	5.6	10.0	6.4	7.9	10.4
CALC. PARAMETERS									
Total dissolved solids	mg/L	202	162	227	181	321	181		179
Charge balance	%	3.88%	5.17%	2.28%	3.26%	0.76%	3.51%	2.29%	1.55%

Table 6-1. (page 3 of 5).

Out-diffusion experiment solution	Units	KFM02B-17	KFM02B-18	KFM02B-19	KFM02B-20	KFM02B-21	KFM02B-22	KFM02B--23	KFM02B-24
SAMPLE DESCRIPTION									
Borehole Length	m	513.34	513.68	514.04	514.47	514.84	515.19	515.54	515.85
Rock Type									
Water-Rock Ratio		0.106	0.108	0.121	0.127	0.113	0.118	0.121	0.114
Experiment Temperature	ºC	45	45	45	45	45	45	45	45
Experiment Time	days	112	112	112	112	112	112	112	112
MISC. PROPERTIES									
Chemical Type		Na-Ca-HCO_3-Cl	Na-Ca-HCO_3-Cl	Na-Ca-HCO_3-Cl	Na-Ca-HCO_3-Cl	Na-Ca-HCO_3-Cl	Na-Ca-HCO_3-Cl	Na-Ca-HCO_3-Cl	Na-Ca-HCO_3-Cl
pH (lab)	-log(H+)	7.12	7.37	7.28	7.42	7.26	7.39	7.44	7.31
Sample Temperature	ºC	20	20	20	20	20	20	20	20
CATIONS									
Sodium (Na^+)	mg/L	35.4	33.4	32.3	35.6	35.1	37.0	36.5	32.4
Potassium (K^+)	mg/L	2.2	1.5	2.7	2.2	1.8	2.2	2.5	1.7
Magnesium (Mg^{+2})	mg/L	<0.3	<0.3	0.3	<0.3	<0.3	<0.3	<0.3	<0.3
Calcium (Ca^{+2})	mg/L	18.6	22.9	25.0	23.3	29.4	26.4	25.1	21.3
Strontium (Sr^{+2})	mg/L	<0.5	<0.5	<0.5	<0.5	<0.5	<0.5	<0.5	<0.5
ANIONS									
Fluoride (F^-)	mg/L	4.7	3.9	4.7	4.4	3.8	4.0	4.7	4.5
Chloride (Cl^-)	mg/L	22.3	23.9	17.1	19.7	19.7	20.5	16.4	20.0
Bromide (Br^-)	mg/L	<0.5	<0.5	<0.5	<0.5	<0.5	<0.5	<0.5	<0.5
Sulphate (SO_4^{-2})	mg/L	3.0	3.0	2.9	2.8	2.9	3.8	3.4	2.8
Nitrate (NO_3^-)	mg/L	2.4	5.1	6.3	5.4	1.0	7.0	6.3	6.5
Total Alkalinity	meq/L	1.44	1.47	1.65	1.76	2.06	1.87	1.94	1.42
NEUTRAL SPECIES									
Aluminium (Al tot)	mg/L	0.093	0.100	0.086	0.100	0.089	0.083	0.081	0.085
Silica (Si)	mg/L	11.9	7.40	12.70	11.80	11.70	10.00	10.90	6.90
CALC. PARAMETERS									
Total dissolved solids	mg/L	174	178	185	195	218	208	207	169
Charge balance	%	2.14%	2.67%	3.66%	1.20%	2.68%	2.17%	1.57%	2.64%

Table 6-1. (page 4 of 5).

Out-diffusion experiment solution	Units	KFM02B-25	KFM02B-26	KFM02B-27	KFM02B-28	KFM02B-29	KFM02B-30	KFM02B--31	KFM02B-32
SAMPLE DESCRIPTION									
Borehole length	m	516.12	516.42	516.72	517.03	517.34	519.54	522.11	522.39
Rock type									
Water-rock ratio		0.120	0.122	0.115	0.110	0.112	0.125	0.118	0.113
Experiment temperature	ºC	45	45	45	45	45	45	45	45
Experiment time	days	112	112	112	112	112	112	112	112
MISC. PROPERTIES									
Chemical type		Na-Ca-HCO_3-Cl	Ca-Na-HCO_3-Cl	Ca-Na-HCO_3-Cl	Ca-Na-HCO_3-Cl	Na-Ca-HCO_3-Cl	Ca-Na-HCO_3-Cl	Na-Ca-HCO_3-Cl	Na-Ca-HCO_3-Cl
pH (lab)	-log(H+)	7.02	7.15	7.16	7.14	7.21	7.14	7.20	7.15
Sample temperature	ºC	20	20	20	20	20	20	20	20
CATIONS									
Sodium (Na^+)	mg/L	35.4	32.5	32.3	36.8	43.2	33.3	41.2	58.4
Potassium (K^+)	mg/L	2.5	4.0	1.8	2.5	1.8	3.0	3.1	2.7
Magnesium (Mg^{+2})	mg/L	0.6	0.3	0.8	<0.3	0.4	0.6	0.7	0.5
Calcium (Ca^{+2})	mg/L	29.6	32.6	32.5	33.1	27.5	34.7	33.6	17.5
Strontium (Sr^{+2})	mg/L	<0.5	<0.5	<0.5	<0.5	<0.5	<0.5	<0.5	<0.5
ANIONS									
Fluoride (F^-)	mg/L	3.7	4.1	3.4	3.1	3.7	4.2	3.9	6.2
Chloride (Cl^-)	mg/L	19.1	18.9	21.2	19.7	22.5	19.9	23.1	25.3
Bromide (Br^-)	mg/L	<0.5	<0.5	<0.5	<0.5	<0.5	<0.5	<0.5	<0.5
Sulphate (SO_4^{-2})	mg/L	3.4	2.4	2.8	3.6	4.1	3.1	4.9	4.7
Nitrate (NO_3^-)	mg/L	11.1	2.1	5.2	9.5	5.2	2.8	9.4	5.1
Total alkalinity	meq/L	1.93	2.20	2.05	2.29	2.28	2.32	2.30	2.15
NEUTRAL SPECIES									
Aluminium (Al tot)	mg/L	0.074	0.080	0.060	0.057	0.057	0.090	0.084	0.087
Silica (Si)	mg/L	11.60	12.50	7.10	7.80	7.00	12.90	14.30	14.60
CALC. PARAMETERS									
Total dissolved solids	mg/L	212	229	219	239	242	240	250	246
Charge balance	%	3.48%	2.13%	2.74%	1.10%	0.65%	1.34%	2.79%	2.23%

Table 6-1. (page 5 of 5).

Out-diffusion experiment solution	Units	KFM02B-33	KFM02B-34	KFM02B-39	KFM02B-40	KFM02B-41	KFM02B-42	KFM02B-43	Blank solution
SAMPLE DESCRIPTION									
Borehole length	m	527.55	532.44	559.83	562.47	565.29	569.35	573.65	
Rock type									
Water-rock ratio		0.117	0.108	0.118	0.116	0.112	0.112	0.112	
Experiment temperature	ºC								
Experiment time	days	112	112	116	116	116	116	116	112
MISC. PROPERTIES									
Chemical type		Na-Ca-HCO_3-Cl	Ca-Na-HCO_3-Cl	Na-Ca-HCO_3-Cl	Na-Ca-HCO_3-Cl	Na-Ca-HCO_3-Cl	Na-Ca-HCO_3-Cl	Na-Ca-HCO_3-Cl	
pH (lab)	-log(H+)	7.27	7.20	6.98	7.22	7.33	7.2	7.28	
Sample temperature	ºC								20
CATIONS									
Sodium (Na^+)	mg/L	60.4	34.5	28.2	42.1	47.4	45.8	40.9	<0.1
Potassium (K^+)	mg/L	3.9	3.2	1.2	2.5	1.8	2.5	2.0	<0.1
Magnesium (Mg^{+2})	mg/L	0.6	1.3	0.3	0.4	<0.3	0.3	0.4	<0.3
Calcium (Ca^{+2})	mg/L	29.3	40.8	9.7	22.0	20.1	16.9	17.6	<0.5
Strontium (Sr^{+2})	mg/L	<0.5	<0.5	<0.5	<0.5	<0.5	<0.5	<0.5	<0.5
ANIONS									
Fluoride (F^-)	mg/L	5.0	3.4	3.6	4.9	4.5	4.9	4.6	<0.5
Chloride (Cl^-)	mg/L	22.3	22.4	20.0	20.7	20.4	22.4	17.0	<0.1
Bromide (Br^-)	mg/L	<0.5	<0.5	<0.5	<0.5	<0.5	<0.5	<0.5	<0.5
Iodide (I)				0.12	0.24	0.45	0.74	0.17	<0.0.5
Sulphate (SO_4^{-2})	mg/L	9.7	11.8	2.1	3.0	2.5	4.0	2.4	<0.5
Nitrate (NO_3^-)	mg/L	2.9	4.3	2.4	0.9	2.2	0.5	0.8	<0.5
Total alkalinity	meq/L	2.96	2.49	0.95	1.99	2.19	1.87	1.94	<0.1
NEUTRAL SPECIES									
Aluminium (Al tot)	mg/L	0.055	0.065	0.061	0.077	0.044	0.061	0.074	<0.01
Silica (Si)	mg/L	15.40	14.40	2.88	10	10.8	9.2	11.5	<0.01
CALC. PARAMETERS									
Total dissolved solids	mg/L	311	268	123	217	230	211	203	<1.0
Charge balance	%	1.60%	0.68%	–0.87%	1.78%	0.29%	0.84%	0.10%	–

6.2 Chloride composition of pore water

Chemically conservative elements such as chloride and bromide are not affected by mineral dissolution because there are no Cl- and Br-bearing minerals present in the rock. Other sources for these elements such as fluid inclusion leakage can also be excluded due to the non-destructive design of the experiment as discussed in /Waber and Smellie 2006b, 2008b/. Therefore, the concentrations of these compounds analysed for the out-diffusion experiment solutions can be converted to *in situ* pore water concentrations using the mass balance calculation given in Equation 3-4.

As shown in the previous pore water investigations and discussed in /Waber and Smellie 2008ab/, the sensitivity of the calculated pore water chloride concentration depends essentially on the accuracy of the determination of the mass of pore water because of its inverse proportionality to the mass of pore water. It was further recognised that the mass of pore water derived from water-content measurements may be influenced by various perturbations, which can result in a deviation of the measured water-content value from that present *in situ*. From previous investigations it was concluded that the applied sample handling and methods to derive the water content, the independency of the methods and the good agreement of the data, indicate that neither stress release nor de-saturation has had a significant effect on the pore water measurements and that the measured and calculated values are representative for *in situ* conditions. Previously, therefore, the uncertainty band of the calculated Cl^- concentration of the pore water was taken as that given by the standard deviation of the multiple water-content measurements.

As described in Chapter 4, in borehole KFM02B additional attempts were undertaken to quantify the effects of potential perturbations of the pore water results by stress release and drilling fluid contamination. This was conducted by drilling the last 15 metres of the borehole with a drilling fluid spiked with 1 g of iodine (added as NaI). The concentration behaviour of I^- was then monitored during the out-diffusion experiments similarily to Cl^-. The detailed results of this study including the modelling of the time series obtained for Cl^- and I^- are given in /Waber et al. in prep./ and summarised in Chapter 4 of this report. Essentially, the perturbations induced by stress release and drilling fluid are within the overall uncertainty band given by the cumulated analytical errors of the different methods, and the obtained pore water Cl^- concentrations confidently represent *in situ* conditions.

Pore-water Cl^- concentrations for the drillcore samples of borehole KFM02B were calculated according to Equation 3-4 and, together with the water content of the large-sized drillcore samples, these were shown to best represent *in situ* conditions. Calculated pore water Cl^- concentrations in most rock matrix samples from borehole KFM02B are below 1,500 mg/kgH_2O and many of them below 1,000 mg/kgH_2O down to the end of the borehole at 574 m borehole length (Table 6-2). Exceptions are samples related to water-conducting zones between about 430–460 m and around 500 m and 520 m borehole length, with Cl^- concentrations up to 3,000 mg/kgH_2O and 2,000 mg/kgH_2O, respectively (Figure 6-4). With such low Cl^- concentrations, the pore waters in the rocks of borehole KFM02B differ from that observed in boreholes KFM01D, KFM06A, KFM08C, and KFM09B drilled in the northwestern part of the Forsmark site /Waber and Smellie 2005, 2007/. Furthermore, in these boreholes the Cl^- concentrations of the pore water generally increase with increasing depth. This is not the case for borehole KFM02B where elevated Cl^- concentrations are associated with highly transmissive water-conducting zones, but not with depth.

Pore water samples with Cl^- concentrations above 1,500 mg/kgH_2O occur in the near-vicinity of high frequencies of highly transmissive fractures between 410–450 m, 470–472 m, and 500–502 m borehole length (Figure 6-4). In contrast, lowest Cl^- concentrations at 490 m (642 mg/kgH_2O), 509 m (893 mg/kgH_2O) and 569 m (781 mg/kgH_2O) borehole length, generally occur at greater distances to water-conductive fractures which are also orders of magnitude less transmissive than those mentioned for high Cl^- concentrations. Indeed, no flowing fractures could be identified below 502 m borehole length although a significant anomaly occurs in the caliper and single point resistance logs at 510 m borehole length /Väisäsvaara and Pöllänen, 2007/. Just below that depth, the Cl^- concentrations once again show large variations over short distances (Figure 6-5). This suggests the presence of a near-by water-conducting fracture that might not have been resolved by the flow logging. Alternatively, near-by water-conducting zones might simply have been missed by the borehole, thus highlighting once more the restriction of borehole investigations to roughly one-dimension. No differential flow logging could be performed due to instrumental limitations in the last about 6 m of the borehole (568–573.87 m borehole length), i.e. the lower part where the drilling-fluid tracer experiment was conducted.

Table 6-2. KFM02B borehole: Chloride concentrations of pore water.

Laboratory sample No	Borehole length (m)	Lithology	Pore water Cl (mg/kg H_2O)	Pore water Cl – error [1] (mg/kg H_2O)	Pore water Cl + error [1] (mg/kg H_2O)
KFM02B-1	158.91		1,092	98	120
KFM02B-2	171.83		1,082	96	117
KFM02B-3	210.64		1,009	90	110
KFM02B-4	287.16		1,226	109	134
KFM02B-5	393.29		1,008	90	110
KFM02B-6	430.74		2,884	259	316
KFM02B-7	441.45		1,910	171	208
KFM02B-8	448.06		2,787	249	304
KFM02B-9	459.84		2,904	260	318
KFM02B-10	474.07		1,415	126	154
KFM02B-11	478.89		963	86	105
KFM02B-12	490.46		642	57	70
KFM02B-13	498.84		1,888	166	203
KFM02B-14	509.81		893	79	97
KFM02B-15	512.57		968	86	106
KFM02B-16	512.96		1,644	148	180
KFM02B-17	513.34		1,411	126	154
KFM02B-18	513.68		1,135	101	124
KFM02B-19	514.04		1,092	98	120
KFM02B-20	514.47		1,241	111	136
KFM02B-21	514.84		972	87	106
KFM02B-22	515.19		1,024	91	111
KFM02B-23	515.54		924	83	101
KFM02B-24	515.85		1,188	106	130
KFM02B-25	516.12		1,162	104	127
KFM02B-26	516.42		1,243	111	136
KFM02B-27	516.72		985	88	107
KFM02B-28	517.03		947	84	103
KFM02B-29	517.34		945	84	103
KFM02B-30	519.54		1,429	128	157
KFM02B-31	522.11		1,731	155	190
KFM02B-32	522.39		1,811	162	198
KFM02B-33	527.55		1,082	96	118
KFM02B-34	532.44		1,362	122	149
KFM02B-39	559.83		1,014	90	110
KFM02B-40	562.47		1,018	91	111
KFM02B-41	565.29		974	87	106
KFM02B-42	569.35		781	69	84
KFM02B-43	573.65		926	83	101

[1] Error based on the standard deviation of multiple water-loss measurements.
Borehole length values represent preliminary borehole data when sampled in the field.

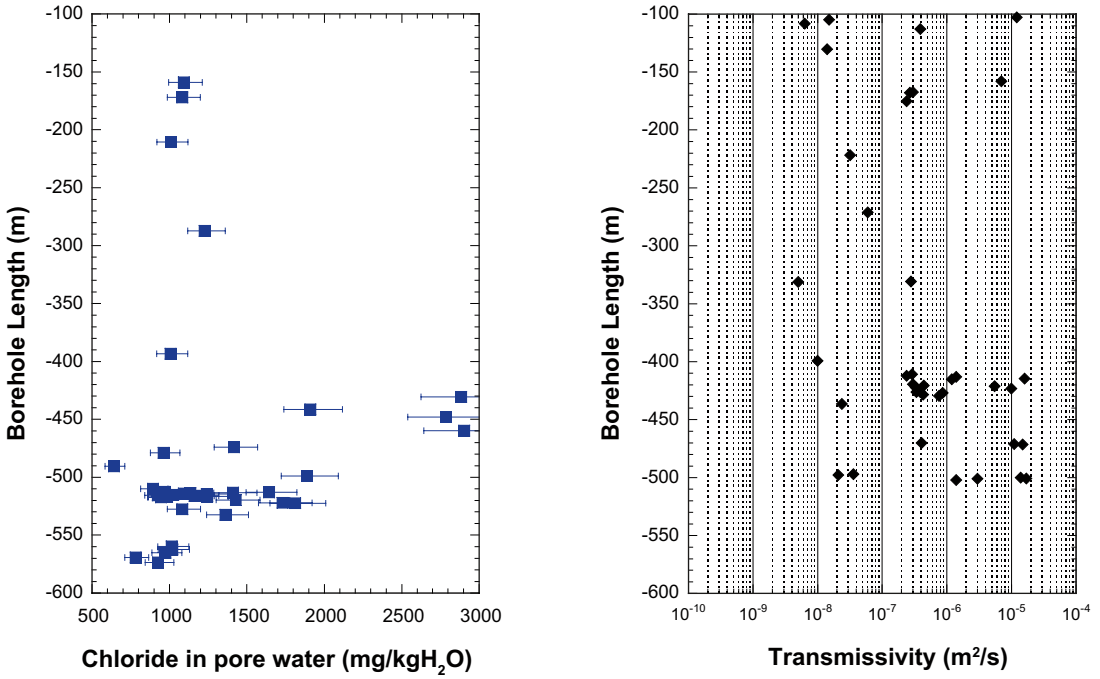

Figure 6-4. *Borehole KFM02B: Chloride concentration of pore water as a function of sampling depth (left) compared to the measured hydraulic transmissivity of all detected water-conducting fractures (right, data from /Väisäsvaara and Pöllänen 2007/).*

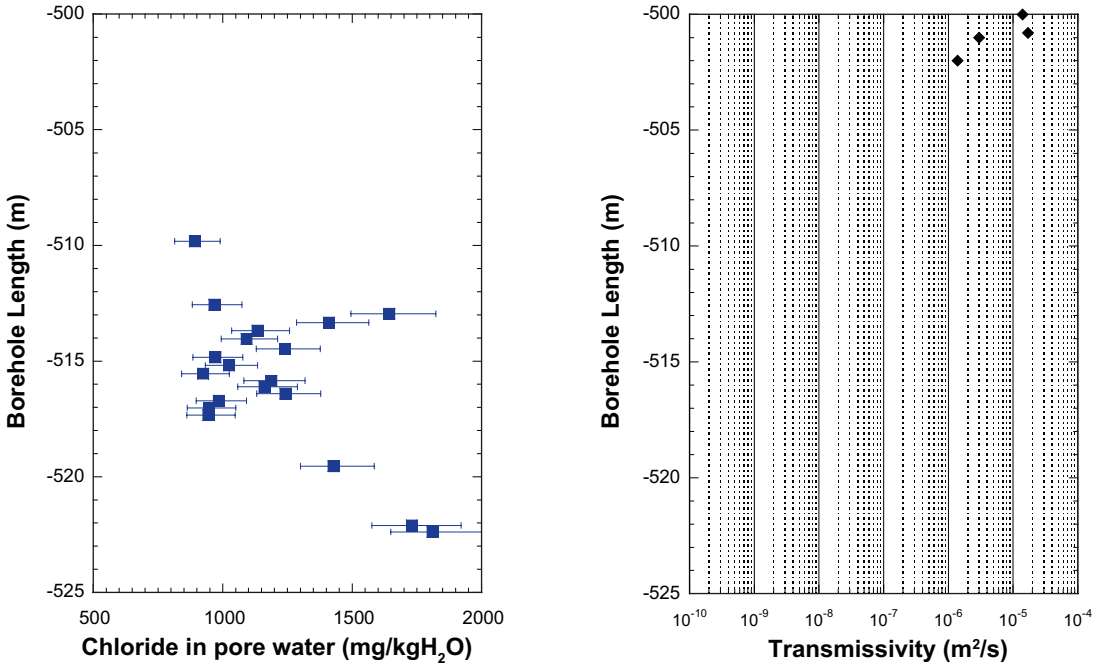

Figure 6-5. *Borehole KFM02B: Chloride concentrations of pore water in samples continuously collected along a profile at 512 m (left), which, however, missed the important detected water-conducting fractures by about 10 metres (right, data from /Väisäsvaara and Pöllänen 2007/).*

Unfortunately, one of the objectives of the pore water investigations in borehole KFM02B was not met, namely the continuous sampling of drillcore in deformation zone ZFMF1 from a highly transmissive fracture into the intact rock matrix, i.e. a so-called fracture profile. The close-up of the depth profile is illustrated in Figure 6-5 where it can be seen that pore water sampling commenced about 10 metres too far into the surrounding rock matrix (i.e. at 512 m borehole length) from the lower intercept of the highly transmissive fractures located between 500–502 m borehole length.

6.3 Other evidence for the chemical composition of pore water

With a few fracture-related exceptions, pore water in the rocks of borehole KFM02B have low Cl^- concentrations down to great depth which contrasts with the observations made in the other boreholes from the Forsmark site /Waber and Smellie 2005, 2007/. However, the apparently dilute pore water differs also in other aspects from those in the other boreholes. Most pronounced are the elevated Mg^{2+} concentrations that were measured for several experiment solutions (Table 6-1). This differs markedly from the out-diffusion experiment solutions of the other boreholes where magnesium could hardly be detected. In Section 6.2 it was shown that the contribution of Mg^{2+} from mineral dissolution reactions is low and that the Mg^{2+} concentrations of the experiment solution might be converted to apparent pore water concentrations in a similar way as the Cl^- concentrations. As shown in Figure 6-6, a positive correlation results between Cl^- and apparent Mg^{2+} concentrations in the pore water. Highest concentrations of Mg^{2+} occur in the same intervals as the Cl^- concentrations exceed 1,500 mg/kgH_2O, i.e. between 410–450 m and 500–502 m (Figure 6-7). In addition, elevated Mg^{2+} concentrations also occur combined with lower Cl^- concentrations in the shallow levels down to about 400 m and also between about 510–530 m borehole length. In samples with the lowest Cl^- concentrations at 490 m, 509 m, and 569 m, the Mg^{2+} concentrations are at or below detection limit.

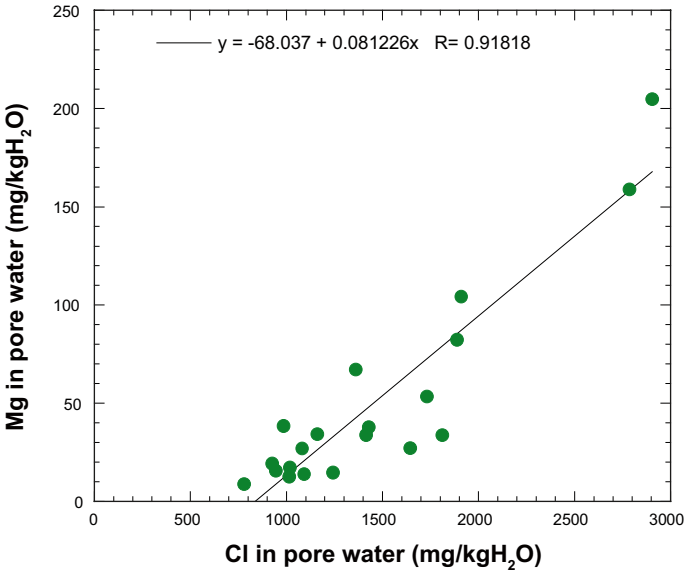

Figure 6-6. *Borehole KFM02B: Apparent concentrations of Mg^{2+} in pore waters as a function of Cl^- concentrations in pore water. Note the general positive correlation in spite of the non-conservative behaviour of Mg^{2+} during the out-diffusion experiments (see text).*

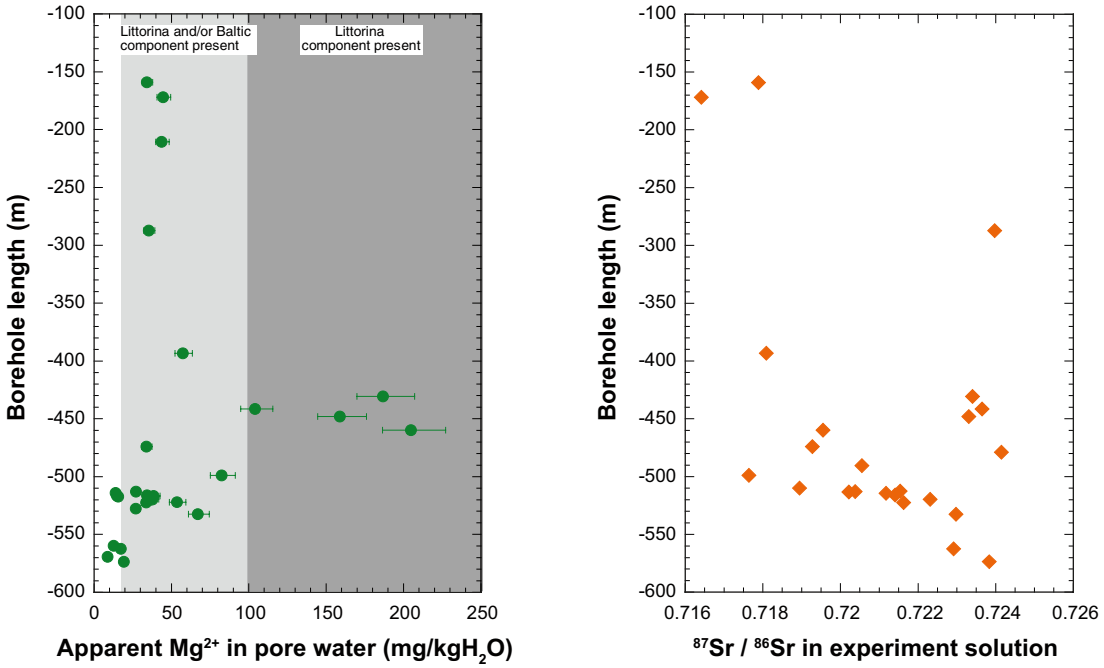

Figure 6-7. *Borehole KFM02B: Apparent concentration of Mg^{2+} in pore water (left) and the $^{87}Sr/^{86}Sr$ ratio of the out-diffusion experiment solution (right) as a function of sampling depth. Note that neither Mg^{2+} nor Sr^{2+} behave conservatively during the out-diffusion experiments (see text).*

In the fracture groundwaters, high Mg^{2+} concentrations are indicative for brackish marine waters (e.g. Littorina and/or Baltic Sea water influence) /SKB 2007/. The roughly extrapolated Mg^{2+} concentrations should not be mistaken for absolute pore water concentrations. Nevertheless, and in combination with the Cl-concentrations, such Mg^{2+} values above 100 mg/kgH_2O might well indicate the presence of a Littorina component in these pore waters, whereas values between about 20–100 mg/kgH_2O might be more indicative for a Littorina and/or a Baltic Sea water component. As shown in Section 6.4, such an interpretation is also consistent with the composition of the water isotopes of the pore water, although it is not possible to differentiate between Littorina and Baltic Sea water due to the very similar isotope composition of these end members /SKB 2007/. In order to do so, other chemical and isotopic indicators are necessary, and/or the exact knowledge of the fracture water composition as a function of time and distance to the next water-conducting fracture, to allow a distinction between these water types via modelling of the exchange between pore water and fracture water.

The pore water in the rocks of borehole KFM02B also differs in their Sr-concentration from, for example, borehole KFM06A. In this latter borehole, two different trends were observed between Cl^- or/and $^{87}Sr/^{86}Sr$ and Sr^{2+} in the experiment solutions for shallow to intermediate samples and deep-seated samples in spite of the non-conservative behaviour of Sr^{2+} during the out-diffusion experiment /Waber and Smellie 2005/. In the experiment solutions of the KFM02B samples no such correlations are established and the Sr^{2+} concentrations are generally lower. The $^{87}Sr/^{86}Sr$ ratios, in turn, cover about the same range as the experiment solutions from borehole KFM06A. Greatest differences in the $^{87}Sr/^{86}Sr$ ratio are similarly related to water-conducting zones as for Cl^- and Mg^{2+} (Figure 6-7).

6.4 Water isotope composition of pore water

The water isotope compositions of the pore water, expressed as $\delta^{18}O$ and $\delta^{2}H$ relative to V-SMOW, were derived by the diffusive isotope exchange technique. As shown by /Rübel 2000/, the uncertainty of the derived values and the calculated mass of pore water and pore water isotope composition is mainly sensitive to the ratio of pore water to test water used in the

experiment. Within the Forsmark site investigation programme, this technique was continuously improved upon and the error could be significantly reduced compared to the samples form the first study performed on material from borehole KFM06A /Waber and Smellie 2005/.

The oxygen and hydrogen isotope composition of pore water in rock samples from borehole KFM02B plot over a wide range of isotope compositions mainly parallel to the Global Meteoric Water Line, GMWL, along a line given by the proposed end member fracture water compositions (see /SKB 2007/). Most samples have isotope compositions between that of the end-member compositions of sea water and present-day infiltration (Figure 6-8). However, several samples are depleted in ^{18}O and ^{2}H and plot between present-day infiltration and the glacial reference water indicating the presence of a cold climate and/or glacial component in these pore waters.

The most depleted isotope composition with a $\delta^{18}O$ value of –14.7‰ and a $\delta^{2}H$ value of –120 ‰ is displayed by the shallowest sample at 171.8 m borehole length (sample 2B-2; Table 6-3) indicating the presence of a cold climate and/or glacial component in this pore water. Below around 200 m the isotope signatures become enriched in ^{18}O and ^{2}H with $\delta^{18}O$ and $\delta^{2}H$ values between those of Baltic Sea water and present-day (summer) meteoric water (Figure 6-9). Down to about 440 m borehole length (sample 2B-7), the water isotope signatures become increasingly depleted in ^{18}O and ^{2}H towards cold climate-type signatures. In one dimension, all these samples are between 5–10 metres away from the next water-conducting fracture with a transmissivity of about 10^{-8} m^2/s. The exception is sample 2B-6 (430 m of depth) which is located only about 1 metre away from a fracture with a transmissivity of about 10^{-5} m^2/s, but unfortunately no isotope composition is available due to either a failure during the experiment or the analyses. Between 410–450 m borehole length at the intersection of borehole KFM02B with the deformation zone ZFMA2, and where an increased frequency of highly transmissive fractures occur with the highest recorded Cl^- and apparent Mg^{2+} concentrations in the pore water (cf. Figures 6-4 and 6-7), the isotope composition of the pore water becomes again enriched in ^{18}O and ^{2}H (Figure 6-9). Although the variation is large at least two samples show isotope compositions similar to that of brackish marine water (Littorina and/or Baltic Sea water).

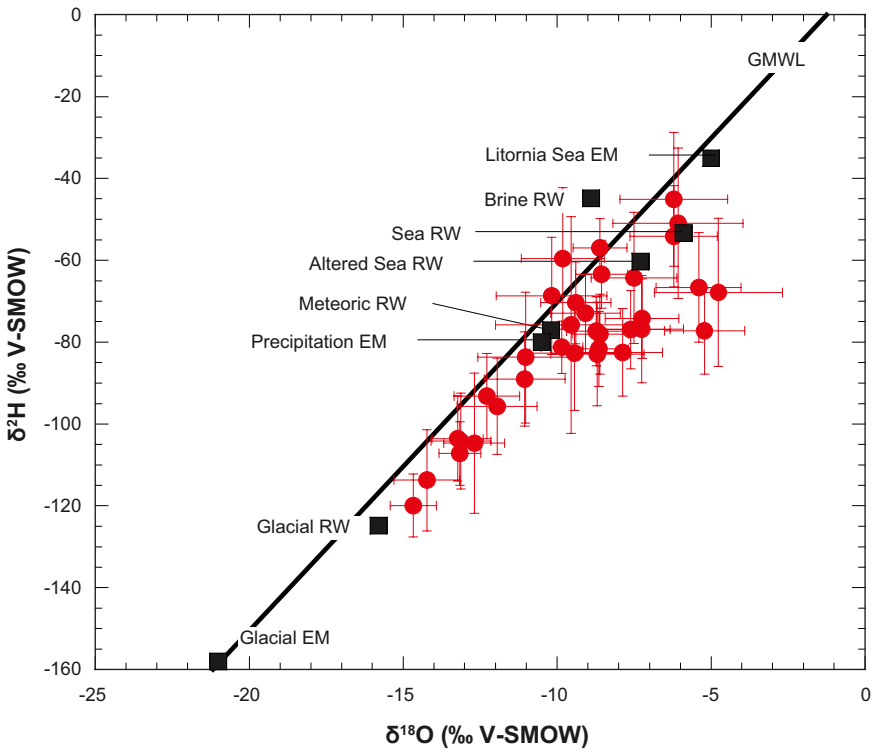

Figure 6-8. *Borehole KFM02B: $\delta^{18}O$ and $\delta^{2}H$ values of pore water compared to the GMWL, and the isotopic composition of proposed end members (EM) and reference water (RW) compositions of various Swedish groundwaters (data from /SKB 2007/). Error bars indicate cumulated error calculated with Gauss' law of error propagation.*

Table 6-3. KFM02B borehole: $\delta^{18}O$ and $\delta^{2}H$ of pore water.

Laboratory sample No	Borehole Length (m)	$\delta^{18}O$ [1] pore water (‰ V–SMOW)	Absolute error $\delta^{18}O$ [1] (‰ V–SMOW)	$\delta^{2}H$ [1] pore water (‰ V–SMOW)	Absolute error $\delta^{2}H$ [1] (‰ V-SMOW)
KFM02B-1	158.91	– [2]		– [2]	
KFM02B-2	171.83	–14.67	0.7	–119.9	7.6
KFM02B-3	210.64	–7.61	1.3	–76.9	9.6
KFM02B-4	287.16	–8.73	1.0	–77.4	8.4
KFM02B-5	393.29	–11.05	1.3	–89.0	11.5
KFM02B-6	430.74	– [3]		– [3]	
KFM02B-7	441.45	–12.28	1.1	–93.2	10.4
KFM02B-8	448.06	–7.25	1.2	–74.2	9.7
KFM02B-9	459.84	–5.40	1.4	–66.6	13.4
KFM02B-10	474.07	–8.69	1.5	–82.9	12.6
KFM02B-11	478.89	–10.18	1.8	–68.7	14.4
KFM02B-12	490.46	–14.23	1.1	–113.8	12.4
KFM02B-13	498.84	–8.61	0.9	–56.9	7.1
KFM02B-14	509.81	–13.15	0.7	–107.2	7.8
KFM02B-15	512.57	–13.23	0.8	–103.6	10.4
KFM02B-16	512.96	–9.81	1.3	–59.6	17.3
KFM02B-17	513.34	–11.95	1.3	–95.7	11.8
KFM02B-18	513.68	–8.61	0.9	–78.0	9.8
KFM02B-19	514.04	–9.43	1.5	–82.7	14.0
KFM02B-20	514.47	– [3]		– [3]	
KFM02B-21	514.84	–7.88	1.3	–82.5	10.7
KFM02B-22	515.19	–7.25	1.3	–76.8	13.1
KFM02B-23	515.54	–4.76	2.1	–67.8	18.1
KFM02B-24	515.85	–6.77	2.1	– [3]	
KFM02B-25	516.12	–5.21	1.3	–77.3	10.5
KFM02B-26	516.42	–8.65	1.0	–81.7	9.2
KFM02B-27	516.72	–9.40	1.1	–70.4	10.0
KFM02B-28	517.03	–8.56	0.8	–63.4	8.3
KFM02B-29	517.34	–9.08	1.1	–72.9	9.6
KFM02B-30	519.54	–7.50	1.4	–64.3	16.0
KFM02B-31	522.11	–9.55	2.5	–75.8	26.5
KFM02B-32	522.39	–9.85	0.7	–81.3	6.4
KFM02B-33	527.55	–11.03	1.5	–83.7	16.0
KFM02B-34	532.44	– [3]		– [3]	
KFM02B-39	559.83	–6.21	1.8	–45.1	16.4
KFM02B-40	562.47	–6.21	1.4	–54.1	12.3
KFM02B-41	565.29	–13.12	1.0	–104.2	11.8
KFM02B-42	569.35	–12.69	1.0	–104.7	17.1
KFM02B-43	573.65	–6.08	2.1	–51.0	18.4

[1] Error calculated with Gauss' law of error propagation.
[2] Too little material to perform the experiment
[3] Meaningless isotope analysis due to evaporation/condensation processes.
Borehole length values represent preliminary borehole data when sampled in the field.

Large variations in the pore water isotope composition are also observed at the intersection of borehole KFM02B with deformation zone ZFMF1 and its associated.

Large variations in the pore water isotope composition are also observed at the intersection of borehole KFM02B with deformation zone ZFMF1 and its associated high frequency of highly conducting fractures starting from about 490 m of borehole length (Figure 6-9). Within short distances cold temperature to glacial isotope signatures with $\delta^{18}O$ and $\delta^{2}H$ values between about –13‰ to –14.5‰ and –105‰ to –114‰ alternate with brackish marine-type signatures similar to those of Littorina and Baltic seawater. Close examination of the data reveals that such variations are repeated three times where the distance along the borehole to the next water-conducting fracture is within a few metres only. The most negative isotope compositions occur at borehole lengths of 490 m, 509–512 m, and 565–569 m and coincide with the lowest Cl^{-} concentrations and the lowest or non-detectable apparent Mg^{2+} contents. At each of these locations, the gradients described by the pore water isotope compositions are steep and the transition from cold temperature glacial-type to brackish marine-type isotope signatures occurs within some decimetres to a few metres.

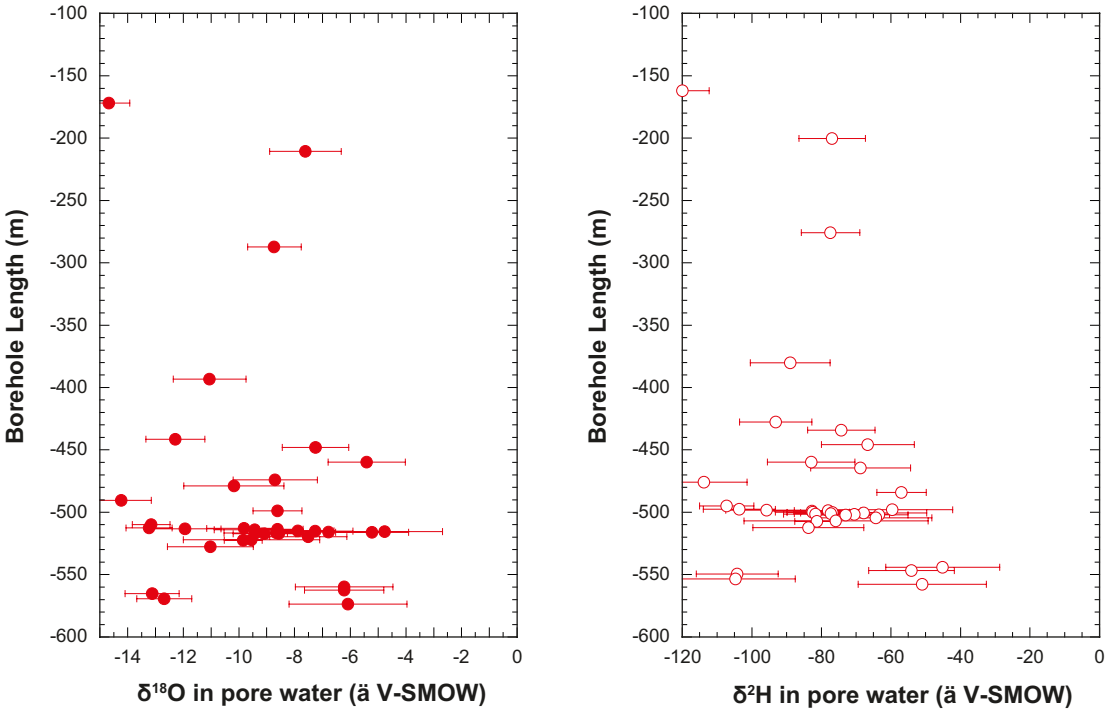

Figure 6-9. *Borehole KFM02B: Depth variation of $\delta^{18}O$ and $\delta^{2}H$ in pore waters. Error bars indicate cumulated error calculated with Gauss' law of error propagation.*

7 Discussion

The pore water investigations performed on core samples from borehole KFM02B demonstrate that the considerable logistic effort to sample drillcore material in its original saturated state was greatly worthwhile. Furthermore, the results of the drilling fluid contamination study performed are in strong support that the pore water data obtained by the present indirect methods are representative for *in situ* conditions to a high degree. The indirect methods applied to drillcores drilled with spiked drilling fluid and the modelling of the obtained data reveal that the contamination induced during drilling is negligible (less than 1%). For the bedrock of the Forsmark site, the contamination induced by stress release is less than about 8% and is therefore well within the uncertainty band of the cumulated error of the applied experimental and analytical methods. In conclusion, the produced data can be regarded as representative for *in situ* conditions. This also justifies a more extensive usage of the data for the palaeohydrogeological interpretation of the Forsmark site.

Unlike previous boreholes, the sampling of drillcore sections for pore water investigations in borehole KFM02B was not only restricted to extended portions of intact rock matrix, but also the rock matrix in the vicinity of the highly fractured deformation zones. Obviously, this limits the value of any depth trends observed for water content and water-loss porosity data used to assess possible perturbations by stress release and similar perturbations. Yet, neither the water content nor the water-loss porosity of the drillcore samples of borehole KFM02B show a trend other than being correlated to the degree of rock deformation and alteration. Indeed, if only samples far from such zones would be considered, then a decrease in these properties with increasing depth would be established, as already suggested by samples from the previous boreholes /Waber and Smellie 2005, 2007/. Thus, the bulk of petrophysical data obtained for drillcore material from borehole KFM02B also appear to represent *in situ* conditions.

In spite of the failure to sample a continuous fracture profile, the correlation of chemical and isotope composition of the pore waters between the sample and the next water-conducting fracture reveals some insight to the palaeohydrogeological evolution of the metagranite encountered in borehole KFM02B, and thus of the hanging wall (target) area of the Forsmark site. Borehole KFM02B intersected deformation zone ZFMA2 at about 420 m borehole length and deformation zone ZFMF1 at about 490 m. Both these deformation zones are characterised by a high frequency of water-conducting fractures which is reflected in the pore water composition. Pore waters from borehole KFM02B have very low Cl-concentrations (less than 1,000 mg/kg H_2O) down to a much greater depth at about 570 metres compared to pore waters of the footwall area (i.e. boreholes KFM01D, KFM08C, KFM09B, and lower part of KFM06A). Indeed, there are only a few samples with more than 2,000 mg/kg H_2O and most samples from 150 m down to the end of the borehole at about 574 m have Cl^- concentrations of less than 1,500 mg/kg H_2O. The low Cl^- concentrations are combined with $\delta^{18}O$ and $\delta^{2}H$ values that plot along a line representing known reference and end-member fracture groundwater types parallel to the GMWL, and show a variation between glacial to cold-climate and brackish marine-type signatures. Such extreme changes occur at least within three intervals at about 470–490 m, 502–520 m and 560–574 m borehole length, all of them representing highly fractured zones with an elevated transmissivity. At each of these locations the chemical and isotopic gradients described by the pore water are steep which is typical for (geologically) short-term changes in the boundary conditions, i.e. in the fracture water composition.

The lowest Cl^- concentrations of less than 1,000 mg/kg H_2O correlate with the most depleted isotope compositions with $\delta^{18}O$ values of less than –13‰ and $\delta^{2}H$ values of less than –105‰ V-SMOW at depths of 490 m, 509–512 m, and 565–569 m borehole length. These samples are located within a distance of about 10 metres to the next highly conductive fracture, although there are no hydraulic data available for the last interval at 565–569 m borehole length. The experiment solutions of these samples are further characterised by Mg^{2+} concentrations around or below detection, indicating low Mg^{2+} concentrations in the pore water. All these characteristics are consistent with a large component of cold-temperature glacial infiltration being present in these pore waters.

In turn, the highest Cl^- concentrations greater than 1,500 mg/kg H_2O correlate with the most enriched isotope composition with $\delta^{18}O$ values of between about –7.5‰ to –5‰ and δ^2H values of between about –70‰ to –45‰ V-SMOW at depths of 430–460 m and around 500 m and 520 m borehole length. In one dimension, these samples are located within a distance of less than 10 metres to the next highly conductive fracture, with most of them being closer than 5 m. The experiment solutions of these samples have elevated Mg^{2+} concentrations, which would convert to pore water concentrations of more than 50 mg/kg H_2O when taking into account the non-conservative behaviour of Mg^{2+} during the out-diffusion experiment. For samples between the 430–460 m borehole length interval, the pore water Mg^{2+} concentrations appear to be even higher than about 150 mg/kg H_2O. This combined evidence thus reveals that within these intervals the pore water consists to a large degree of a brackish marine component. Indications for a large Littornia seawater component are certainly present for the 430–460 m interval based on the suggested high Mg^{2+} concentrations, whereas the distinction between Littorina and Baltic seawater component in the other samples is hardly possible without detailed evaluation coupled to geochemical and transport modelling.

To conclude, the pore water investigations performed on rock matrix material from borehole KFM02B indicate that especially in the catchment areas of deformation zone ZFMA2 and ZFMF1, the hanging wall bedrock in this area represents a hydraulically much more dynamic system than previously observed for the footwall bedrock in the northwestern part of the Forsmark site area. The Cl^- concentrations are mainly below 1,500 mg/kg H_2O from shallow to great depth. Higher Cl^- concentrations up to a maximum of about 3,000 mg/kg H_2O are related to water-conducting fractures within deformation zones ZFMA2 and ZFMF1 and, in combination with the isotope composition and Mg^{2+} concentrations, indicate the presence of large components of brackish marine-type water (Littorina and/or Baltic seawater). From below 150 m, the isotopic signatures become typical of cold climate (glacial?) infiltration, and then change below around 200 m borehole length to values enriched in ^{18}O and ^2H still associated with low Cl^- concentrations. Down to about 420 m borehole length the oxygen isotope signatures become increasingly depleted in ^{18}O and ^2H towards cold climate, glacial-type signatures. In discrete zones related to conductive fractures, such signatures depleted in ^{18}O and ^2H and associated with the lowest Cl^- concentrations occur down to 565 m borehole length indicating that in these fractures cold climate, glacial-type groundwater must have circulated prior to the groundwaters sampled today.

8 Acknowledgements

Much appreciation is given to Kenneth Åkerström (SKB) for the on-site selection and packaging and rapid dispatching of the drillcore samples to the University of Bern. The support and patience of Anne-Chatrin Nilsson (SKB) throughout the study is much appreciated. We are grateful for the analytical support from R Maeder, F Eichinger, and G Chevalier (solution chemistry) at the Institute of Geological Sciences, University of Bern.

9 References

Carlsten S, Döse C, Samuelsson E, Gustafsson J, Petersson J, Stephens M, Thunehed H, 2007. Forsmark site investigations. Geological single-hole interpretation of KFM02B. SKB P-07-107, Svensk Kärnbränslehantering AB.

Liedberg L, 2006. Forsmark site investigation: Borehole KFM01A, KFM01C, KFM01D, KFM04A, KFM05A and KFM06A. Determination of porosity by water saturation and density by buoyancy technique. SKB P-06-234, Svensk Kärnbränslehantering AB.

Parkhurst D L, Appelo C A J, 1999. User's Guide to PHREEQC (Version 2) – A Computer Program for Speciation, Batch-Reaction, One-Dimensional Transport, and Inverse Geochemical Calculations: Denver, CO, U. S. Geological Survey, Water-Resources Investigations Report 99-4259; v. 2–15, 2008.

Pearson F J, Arcos D, Bath A, Boisson J Y, Fernandez A M, Gaebler H-E, Gaucher E C, Gautschi A, Griffault L, Hernan P, Waber H N, 2003. Mont Terri Project – Geochemistry of Water in the Opalinus Clay Formation at the Mont Terri Rock Laboratory. Reports of the Federal Office of Water and Geology (FOWG), Geology Series No. 5, Bern, Switzerland.

Rübel A P, 2000. Stofftransport in undruchlässigen Gesteinsschichten – Isotopenuntersuchungen im Grund- und Porenwasser. PhD Thesis, Institut für Umweltphysik, Unversity of Heidelberg, Der Andere Verlag, Osnabrück, Germany.

Samuelsson E, Dahlin P, Lundberg E, 2007. Forsmark site investigation. Boremap mapping of telescopic drilled borehole KFM02B. SKB P-07-102, Svensk Kärnbränslehantering AB.

SKB, 2007. Hydrochemical evaluation of the Forsmark site, modeling stage 2.1 – issue report. SKB R-06-69), Svensk Kärnbränslehantering AB.

Väisäsvaara J, Pöllänen J, 2007. Forsmark site investigations: Difference flow logging in borehole KFM02B. SKB P-07-83, Svensk Kärnbränslehantering AB.

Waber H N, Smellie J A T, 2005. Forsmark site investigation. Borehole KFM06: Characterisation of pore water. Part I: Diffusion experiments. SKB P-05-196, Svensk Kärnbränslehantering AB.

Waber H N, Smellie J A T, 2006a. Oskarshamn site investigation. Borehole KLX03: Characterisation of pore water. Part 1: Methodology and analytical data. Oskarshamn site investigation. SKB P-06-12, Svensk Kärnbränslehantering AB.

Waber H N, Smellie J A T, 2006b. Oskarshamn site investigation. Borehole KLX03: Characterisation of pore water. Part 2: Rock properties and diffusion experiments. SKB P-06-77, Svensk Kärnbränslehantering AB.

Waber H N, Smellie J A T, 2006c. Oskarshamn site investigation. Borehole KLX08: Characterisation of pore water. Part 1: Methodology and analytical data. Oskarshamn site investigation. SKB P-06-163, Svensk Kärnbränslehantering AB.

Waber H N, Smellie J A T, 2007. Forsmark site investigation. Borehole KFM01D, KFM08C, KFM09B: Characterisation of pore water. Part I: Diffusion experiments and pore water data. SKB P-07-119, Svensk Kärnbränslehantering AB, Stockholm, Sweden.

Waber H N, Smellie J A T, 2008a. Oskarshamn site investigation. Borehole KLX17A: Characterisation of pore water. Part 1: Methodology and analytical data. Oskarshamn site investigation. SKB P-08-43, Svensk Kärnbränslehantering AB.

Waber H N, Smellie J A T, 2008b. Characterisation of pore water in crystalline rocks. Appl. Geochem. 23, 1834-1861.

Waber H N, Gimmi T, Smellie J A T, (in prep.). Pore water in the rock matrix. Site descriptive modelling, SDM Site Forsmark, SKB R-08-105, Svensk Kärnbränslehantering AB.